Paxillin regulates cell polarization and anterograde vesicle trafficking during cell migration

Fatemeh Dubois, Kyle Alpha, and Christopher E. Turner*
Department of Cell and Developmental Biology, State University of New York Upstate Medical University, Syracuse, NY 13210

ABSTRACT **Cell polarization and directed migration play pivotal roles in diverse physiological and pathological processes. Herein, we identify new roles for paxillin-mediated HDAC6 inhibition in regulating key aspects of cell polarization in both two-dimensional and one-dimensional matrix environments. Paxillin, by modulating microtubule acetylation through HDAC6 regulation, was shown to control centrosome and Golgi reorientation toward the leading edge, a hallmark of cell polarization to ensure directed trafficking of promigratory factors. Paxillin was also required for pericentrosomal Golgi localization and centrosome cohesion, independent of its localization to, and role in, focal adhesion signaling. In addition, we provide evidence of an accumulation of paxillin at the centrosome that is dependent on focal adhesion kinase (FAK) and identify an important collaboration between paxillin and FAK signaling in the modulation of microtubule acetylation, as well as centrosome and Golgi organization and polarization. Finally, paxillin was also shown to be required for optimal anterograde vesicular trafficking to the plasma membrane.**

Monitoring Editor
Diane Barber
University of California, San Francisco

Received: Aug 1, 2017
Revised: Sep 26, 2017
Accepted: Oct 13, 2017

INTRODUCTION

The establishment and maintenance of front–rear cell polarity and directed migration is critical during organism development, tissue remodeling, immune surveillance, and wound repair (Ridley *et al.*, 2003). Disruption of cell polarization contributes to the progression of many diseases, including cardiovascular disease, neurodegenerative disorders, tissue fibrosis, and metastatic cancer (Lee and Vasioukhin, 2008). The microtubule (MT) network plays a crucial role in the maintenance of cell architecture and cell polarity. Furthermore, regulated trafficking of vesicles to the cell's leading edge during migration requires an asymmetric distribution of stable MTs (Etienne-Manneville, 2013), which serve as tracks to facilitate directed transport of vesicles containing promigratory factors such as integrins and matrix remodeling enzymes, including metalloproteinases (Mellman and Nelson, 2008; Petrie *et al.*, 2009).

The distribution of MTs is defined mainly by the activities of the centrosome and Golgi complex (Jaffe and Hall, 2005; Bornens, 2012). By nucleating and anchoring MTs, the centrosome and Golgi serve as the two principal MT-organizing centers (MTOCs) in animal cells (Rivero *et al.*, 2009; Rios, 2014; Conduit *et al.*, 2015; Sanders and Kaverina, 2015). Moreover, it has been shown that newly nucleated MTs can become stabilized by posttranslational modifications, such as acetylation on lysine 40 of tubulin (Chabin-Brion *et al.*, 2001; Matsuyama *et al.*, 2002; Matov *et al.*, 2010). Of importance, disruption of MTs by drug treatment or depletion of endogenous MT stabilizers, such as RASSF1A or CLASPs, also perturbs Golgi complex integrity (Hoppeler-Lebel *et al.*, 2007; Miller *et al.*, 2009; Vinogradova *et al.*, 2012; Arnette *et al.*, 2014), as well as centrosome positioning and cohesion (Meraldi and Nigg, 2001; Burakov *et al.*, 2003), further implicating MTs in the maintenance of Golgi and centrosome structure and localization.

This article was published online ahead of print in MBoC in Press (http://www.molbiolcell.org/cgi/doi/10.1091/mbc.E17-08-0488) on October 18, 2017.

*Address correspondence to: Christopher E. Turner (turnerce@upstate.edu).

Abbreviations used: 1D, one-dimensional; 2D, two-dimensional; 3D, three-dimensional; DAPI, 4′,6-diamidino-2-phenylindole; DMSO, dimethyl sulfoxide; ECM, extracellular matrix; ER, endoplasmic reticulum; FA, focal adhesion; FAK, focal adhesion kinase; GFP, green fluorescent protein; HA, hemagglutinin; MFI, mean fluorescence intensity; MT, microtubule; MTOC, MT-organizing center; NA, numerical aperture; PBS, phosphate-buffered saline; PLL, poly-L-lysine; PM, plasma membrane; RNAi, RNA interference; tsVSVG, temperature-sensitive mutant vesicular stomatitis virus G; VSVG, vesicular stomatitis virus G.

© 2017 Dubois *et al.* This article is distributed by The American Society for Cell Biology under license from the author(s). Two months after publication it is available to the public under an Attribution–Noncommercial–Share Alike 3.0 Unported Creative Commons License (http://creativecommons.org/licenses/by-nc-sa/3.0).
"ASCB®," "The American Society for Cell Biology®," and "Molecular Biology of the Cell®" are registered trademarks of The American Society for Cell Biology.

The mechanisms involved in polarized cell motility also have an intimate relationship with focal adhesions (FAs), which are the major sites of cell–extracellular matrix (ECM) interactions (Raghavan *et al.*, 2003; Prager-Khoutorsky *et al.*, 2011). These structures are indispensable for sensing the chemical and mechanical cues in the cell's environment to stimulate the establishment of a distinct leading edge and cell rear (Schneider *et al.*, 2009). Paxillin, a key component of FAs, lacks enzymatic activity but instead functions primarily as a scaffold protein for the assembly of multi-protein complexes to facilitate intracellular signaling (Brown and Turner, 2004; Deakin and Turner, 2008). For example, it has been shown that paxillin, by regulating RhoA- and Rac1-GTPase signaling, can coordinate actin cytoskeleton remodeling and FA turnover to drive cell migration (Webb *et al.*, 2004; Deakin *et al.*, 2012). Recently, we have described a new role for paxillin in regulating MT stability, via interaction with and inhibition of the cytoplasmic deacetylase HDAC6, that in turn controls Golgi organization and directed cell migration (Deakin and Turner, 2014). Importantly, deregulation of HDAC6 activity has been widely associated with increased tumor cell migration and invasion (Aldana-Masangkay and Sakamoto, 2011; Rey *et al.*, 2011; Kanno *et al.*, 2012) as well as with several neurodegenerative disorders (Zhang *et al.*, 2013; Ganai, 2017). However, its mechanism of regulation and action remains poorly understood.

Herein, we identify paxillin as a centrosome-binding protein and provide functional insight into how dynamic, paxillin-regulated post-translational acetylation of MTs via HDAC6 regulation impacts cell polarization by influencing centrosome and Golgi positioning/organization as well as directed MT-dependent vesicle trafficking.

RESULTS

Paxillin-mediated tubulin acetylation is necessary for polarization of the Golgi complex during migration

The reorientation of the Golgi apparatus toward the leading edge of motile cells results in asymmetric distribution of the MT network and is required for polarized trafficking and directional cell migration (Yadav *et al.*, 2009; Hurtado *et al.*, 2011). Recently, we have shown that paxillin plays a major role in regulating Golgi complex integrity via interaction with the deacetylase HDAC6 and modulation of its activity in both normal and transformed cells, including normal human foreskin fibroblasts and MDA-MB-231 breast adenocarcinoma cells (Deakin and Turner, 2014). To gain further insight into the functional consequence of Golgi fragmentation after paxillin knockdown, we first investigated whether paxillin additionally affects Golgi polarization in MDA-MB-231 cells. For this purpose, paxillin was depleted via RNA interference (RNAi) treatment (Figure 1, A and B, and Supplemental Figure S1A), and Golgi positioning was quantified using three different approaches.

A standard scratch wound assay showed paxillin knockdown caused a significant reduction in repositioning of the Golgi apparatus in front of the nucleus at the wound edge, as compared with control cells (Figure 1, C and D), in part because of the associated Golgi fragmentation (Supplemental Figure S1B). As noted previously, paxillin RNAi also induced a significant reduction of acetylated MTs but not total MTs (Supplemental Figure S1C). Therefore, tubacin treatment was used to specifically inhibit HDAC6 activity (Haggarty *et al.*, 2003) and to increase the acetylated tubulin level in an attempt to rescue the paxillin-specific defect (Supplemental Figure S1, C and D; Deakin and Turner, 2014). Interestingly, tubacin treatment rescued not only Golgi complex integrity but also its reorientation at the wound edge in paxillin RNAi-treated cells (Figure 1, C and D).

The formation of a confluent cell monolayer and restrained cell spreading, as in the wound assay, can impact adhesion remodeling and cell polarity (Hale *et al.*, 2011; Burute *et al.*, 2016). Accordingly, we used a micropatterning approach as a complementary method to control the shape and position of individual cells and to establish reproducible polarized cell architecture (Théry, 2010). Cells were plated on either fibronectin-coated crossbow shapes, to generate a defined front and rear, or narrow (2.5- or 5-μm) lines of fibronectin, to mimic the cell morphology and motility more typically observed in three-dimensional (3D) ECM environments and also described as one-dimensional (1D) cell migration (Doyle *et al.*, 2009; Supplemental Figure S1, E and F). Similar to the results of the scratch wound assay, in control RNAi cells, the Golgi complex was compact and localized mostly in front of the nucleus. In contrast, after paxillin depletion, the Golgi was fragmented and randomly dispersed around the nucleus (Figure 1, E–I). Importantly, Golgi cohesion and polarization in front of the nucleus were rescued by inhibition of HDAC6 activity after tubacin treatment (Figure 1, G–I; Deakin and Turner, 2014).

A critical role for paxillin in the regulation of breast cancer cell migration and invasion in which paxillin serves to control directionality, adhesion dynamics, and phenotypic plasticity in both two-dimensional (2D) and 3D ECM microenvironments has previously been described (Deakin and Turner, 2011). To visualize whether paxillin also regulates Golgi positioning during 1D migration on fibronectin lines, MDA-MB-231 cells were infected with baculovirus expressing cyan fluorescent protein (CFP)-nucleus and red fluorescent protein (RFP)-Golgi, and the position of the Golgi in relation to the nucleus was monitored using time-lapse imaging. Control cells displayed a compact polarized Golgi during directional migration for several hours (Figure 1J). In contrast, and consistent with the analysis of fixed cells (Figure 1G), paxillin-depleted cells showed dispersed Golgi structures around the nucleus at all time points, and this was associated with a reduction in migration distance (Figure 1J). Additionally, the majority of the paxillin RNAi-treated cells displayed an elongated phenotype, with no distinct front or rear, as previously observed in paxillin-depleted cells embedded within a 3D ECM (Deakin and Turner, 2011). Together, these data suggest that paxillin regulation of MT acetylation is not only required for Golgi complex cohesion and positioning, but also important for coordinating cell polarization and directed migration.

The proline-rich domain of paxillin is required for Golgi integrity and polarization

We next evaluated the Golgi organization in nontransformed paxillin-null mouse embryonic fibroblasts (paxillin–/– MEFs). These cells also have reduced MT acetylation and a fragmented Golgi complex (Deakin and Turner, 2014). Importantly, reexpression of paxillin tagged with green fluorescent protein (GFP) rescued Golgi integrity, as visualized by GM130 staining (Figure 2, A and B) and MT acetylation (Supplemental Figure S2A).

Paxillin has a well-defined domain structure, with the majority of its interactions with other proteins being mediated by its N-terminus–containing leucine-aspartic acid–rich LD motifs and tyrosine 31 and 118 phosphorylation sites, which are targeted primarily by focal adhesion kinase (FAK) and Src kinases (Supplemental Figure S2B; Brown and Turner, 2004). We therefore used the paxillin–/– MEFs in rescue experiments to pinpoint the paxillin domain(s) responsible for Golgi cohesion and positioning. Accordingly, GFP-paxillin mutants lacking either the LD2 or LD4 motif (the two FAK binding sites; Scheswohl *et al.*, 2008) or the proline-rich domain (HDAC6 binding site; Deakin and Turner, 2014), as well as a nonphosphorylatable (Y31/118F) mutant were expressed in the paxillin–/– MEFs (Brown and Turner, 2004; Deakin and Turner, 2014). In contrast to the other mutants, only the mutant lacking the proline-rich region of paxillin

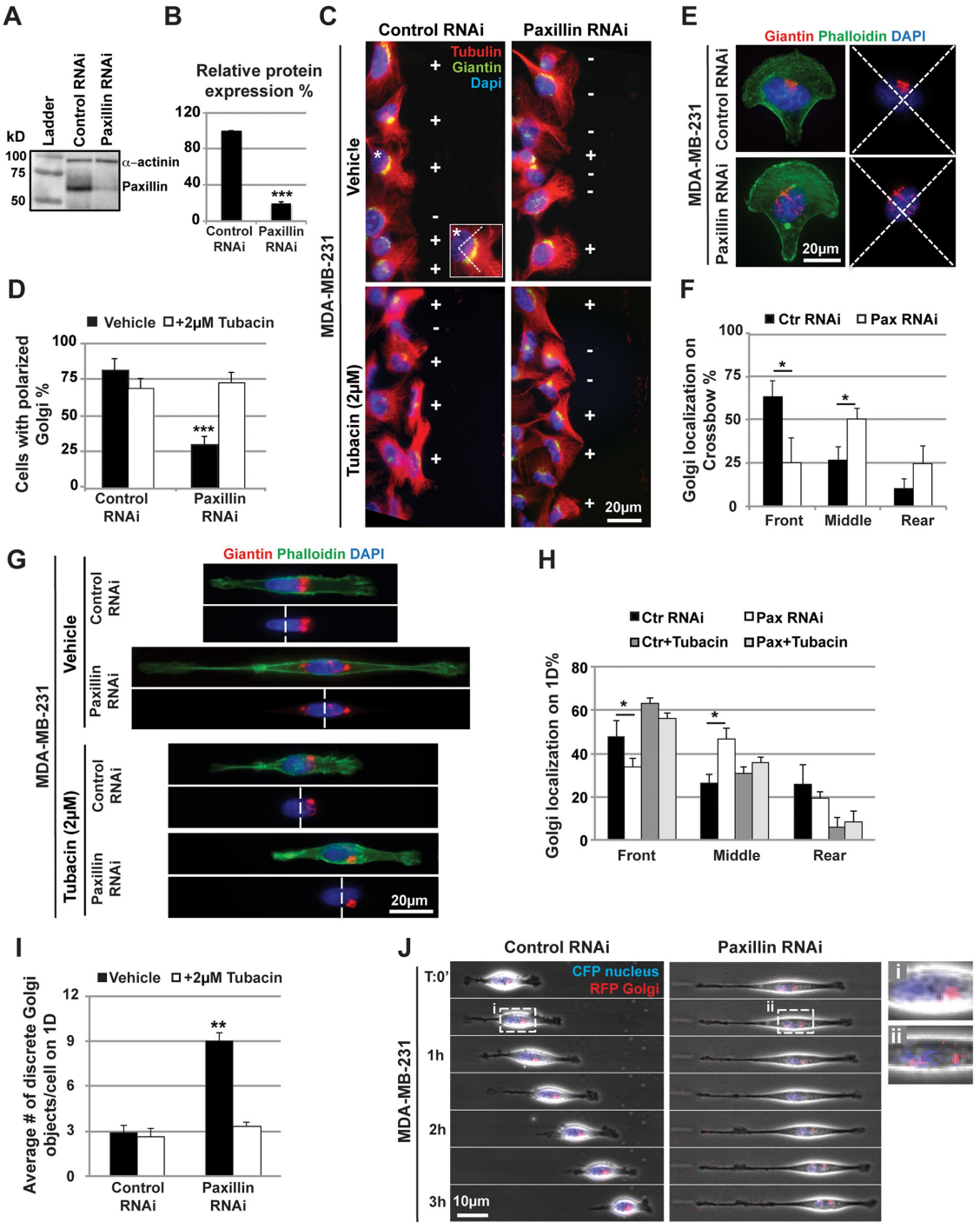

FIGURE 1: Paxillin-mediated tubulin acetylation is necessary for polarization of the Golgi complex during migration. (A) Western blot and (B) quantification indicating the efficiency of paxillin depletion in MDA-MB-231 cells after paxillin RNAi treatment. (C) Representative images and (D) quantification of Golgi polarization 6 h after the monolayer wounding. $n > 100$ cells. The MDA-MB-231 cells were treated with control or paxillin RNAi as indicated and with 2 μM tubacin for 4 h. The Golgi complex was scored as polarized (+) if it was positioned within a 90° sector facing the wound as presented by the cell marked with asterisks. (E) Representative images and (F) quantification of the Golgi localization on the crossbows after RNAi treatment as indicated. $n > 30$ cells. (G) Representative images and (H) quantification of the Golgi localization along with (I) morphometric analysis of discrete Golgi objects on the 1D fibronectin lines (5 μm) after RNAi treatment as indicated and incubation with 2 μM tubacin for 4 h. $n > 100$ cells. See *Materials and Methods* for quantification details. (J) Montage of MDA-MB-231 cell migration on fibronectin-coated lines (5 μm) after treatment with control or paxillin RNAi as indicated, showing Golgi localization (RFP) relative to the nucleus (CFP). Cells were imaged every 10 min for 3 h. Boxed regions used for the zoom. Data are represented as the mean ± SEM from three individual experiments. Statistical significance was determined by Student's *t* test. *$p < 0.05$; **$p < 0.01$; ***$p < 0.001$.

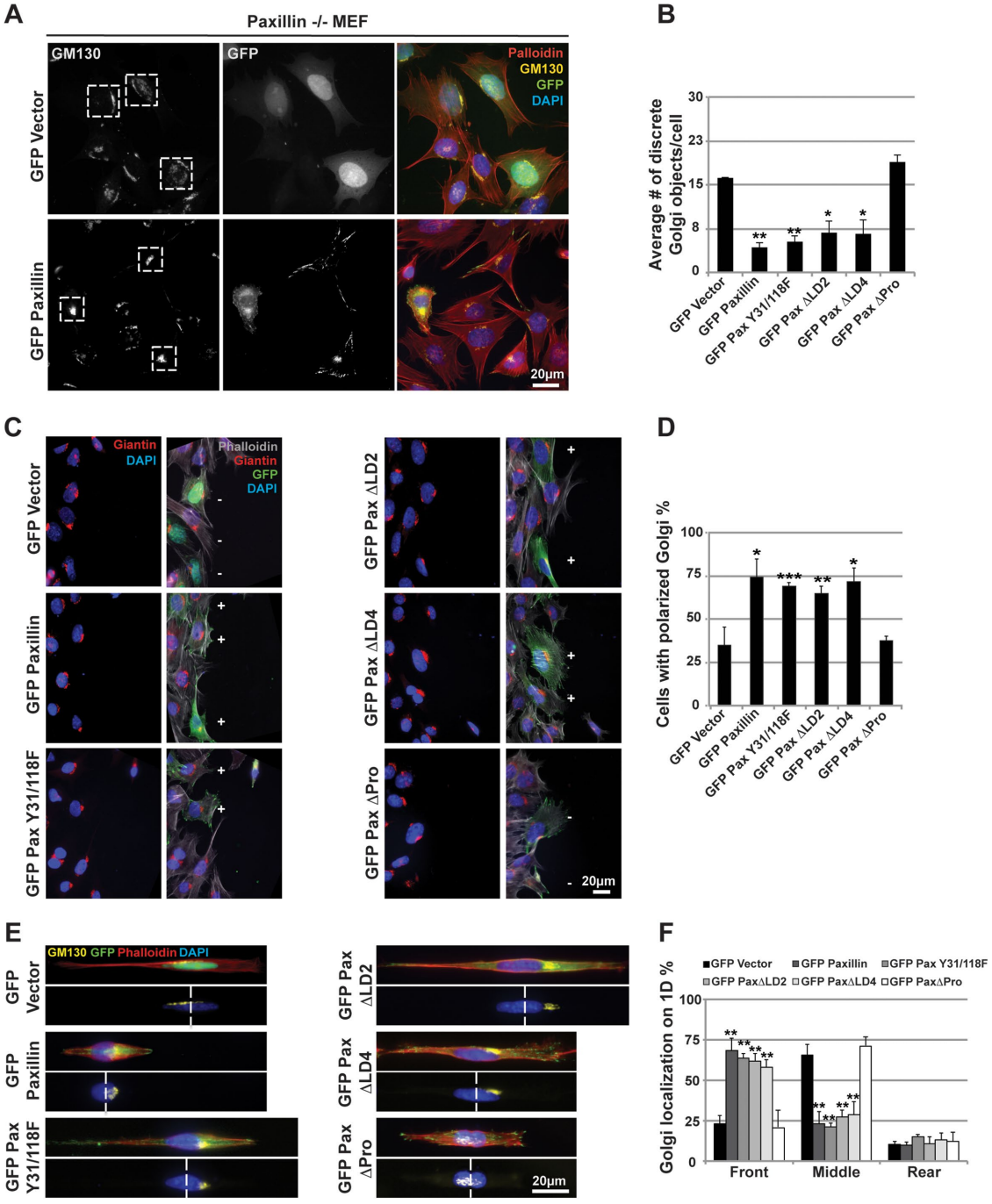

FIGURE 2: The proline-rich domain of paxillin is required for Golgi integrity and polarization. (A) Representative images of Golgi complex (GM130) in paxillin–/– MEFs transfected with GFP-paxillin constructs as indicated for 16 h before fixation. Boxed regions highlight Golgi complex morphology in transfected cells. (B) Quantification of discrete Golgi object number per cell. $n > 30$ cells. (C) Representative images and (D) quantification of Golgi polarization 6 h after monolayer wounding. $n > 100$ cells. The Golgi complex was scored as polarized (+) if it was positioned within a 90° sector facing the wound. (E) Representative images of the Golgi localization on 1D fibronectin lines (5 μm) with (F) morphometric analysis of Golgi polarization in paxillin–/– MEFs transfected with the GFP-paxillin mutants, as described. $n > 50$ cells. See *Materials and Methods* for quantification details. Data are represented as the mean ± SEM from three individual experiments. Statistical significance was determined by Student's *t* test. *$p < 0.05$; **$p < 0.01$; ***$p < 0.001$.

(GFP-paxillin ΔPro) failed to rescue Golgi fragmentation (Figure 2B and Supplemental Figure S2A) and Golgi reorientation either in the scratch wound assay (Figure 2, C and D) or on the fibronectin-coated lines (Figure 2, E and F). It is of note that, as reported previously (Deakin and Turner, 2014), the GFP-paxillin ΔPro mutant was also unable to rescue the level of acetylated tubulin as compared with cells expressing GFP-paxillin wild type or the other paxillin mutants (Supplemental Figure S2A). Taken together, these data indicate that paxillin regulation of Golgi polarization probably involves interaction of its proline-rich domain with HDAC6 (Deakin and Turner,

2014) to inhibit HDAC6 activity and to enhance MT acetylation and stability.

Paxillin is required for pericentrosomal Golgi localization and centrosome cohesion

The centrosome, composed of two centrioles, acts as a major MTOC and is implicated in both the organization and function of the Golgi complex (Rieder *et al.*, 2001; Sütterlin and Colanzi, 2010). The centrosome, by nucleating a radial array of MTs, provides the spatial cue for the assembly of Golgi fragments in its pericentrosomal localization into a single organelle (Thyberg and Moskalewski, 1999; Rivero *et al.*, 2009). Given the functional association between the Golgi and centrosome, we hypothesized that paxillin depletion could also affect pericentrosomal localization of the Golgi apparatus. MDA-MB-231 cells were costained with both centrosome (pericentrin) and the Golgi marker (GM130). In control cells, the Golgi complex remained closely juxtaposed to the centrosome (Figure 3, A and B). However, after paxillin knockdown, two phenotypes were observed. First, the fragmented Golgi was disconnected from the centrosome (Supplemental Figure S3A) by at least 2 µm in ~60% of the cells (Figure 3, A and B), and additionally, loss of centriole cohesion (>1 µm between centrioles) was observed in 43% of paxillin-depleted cells (Figure 3, A and C). To exclude any possible influence of cell cycle stage, which can affect centrosome duplication and Golgi organization, control and paxillin RNAi-treated cells were also analyzed by flow cytometry. No significant differences in either the S or G2/M populations were observed after control versus paxillin RNAi treatment in either asynchronously growing cells (Supplemental Figure S3B) or cells arrested by a double thymidine block (unpublished data). These results demonstrate that the loss of Golgi and centriole cohesion in paxillin-depleted cells was not due to late G2 arrest. Interestingly, both the pericentrosomal localization of the Golgi and centrosome cohesion could be restored in paxillin knockdown cells either by treatment with the HDAC6 inhibitor, tubacin (Figure 3, B and C), or by RNAi-mediated HDAC6 depletion (Supplemental Figure S3, C–I).

Furthermore, to investigate whether paxillin depletion could also influence polarized centrosome localization, control and paxillin RNAi-treated MDA-MB-231 cells were plated and analyzed on 1D fibronectin-coated lines. In the majority of control RNAi-treated cells, the centrosome and Golgi remained connected and polarized in front of the nucleus. In contrast, and similar to the results obtained for Golgi polarization, a significant number of paxillin-depleted cells did not polarize their centrosome and there was also a loss of centriole cohesion (Figure 3, D and E).

Importantly, to further demonstrate a role for elevated HDAC6 activity in the observed phenotypes, parental MDA-MB-231 cells were transfected with either GFP-tagged wild-type HDAC6 or a catalytically inactive (HDAC6 CI) mutant. As with paxillin RNAi, expression of wild-type HDAC6, but not HDAC6 CI, not only decreased the level of acetylated tubulin (Figure 3, F and G) but also caused loss of centriole cohesion (Figure 3, F and H), Golgi fragmentation, and loss of pericentrosomal Golgi localization (Figure 3, I–K). Collectively, these data indicate that paxillin, by modulating MT acetylation via HDAC6, affects the coordinated organization of both the centrosome and Golgi structures.

HDAC6 inhibition, in the absence of paxillin, is able to rescue Golgi and centrosome organization

Analysis of pericentrosomal localization of the Golgi in paxillin–/– MEFs revealed a phenotype similar to that of the paxillin-depleted MDA-MB-231 cells, with the Golgi fragments being separated from their pericentrosomal localization and centriole cohesion being lost (Figure 4, A–C). Expression of the various GFP-paxillin constructs in the paxillin–/– MEFs further demonstrated a requirement for the proline-rich region. Only GFP-paxillin ΔPro mutant–expressing cells failed to rescue the pericentrosomal Golgi complex organization and centriole cohesion (Figure 4, A–C), which was also associated with failure to rescue normal acetylated tubulin levels (Supplemental Figure S2A). Moreover, the cells transfected with the GFP-paxillin ΔPro mutant showed a loss of centrosomal polarization on fibronectin-coated lines (Supplemental Figure S4, A and B).

Importantly, expression of the catalytically inactive HDAC6 CI mutant in paxillin–/– MEFs not only increased the acetylated tubulin level as compared with cells transfected with GFP-vector (Figure 4, D and E), but also rescued separation of centrioles (Figure 4, D and F) as well as Golgi pericentrosomal localization and cohesion (Figure 4, G–I). These data therefore confirm the requirement of the proline-rich region of paxillin for control of HDAC6-regulated MT acetylation and highlight the importance of this signaling axis in the regulation of Golgi and centrosome organization.

Phosphorylation of cytosolic paxillin is necessary for centrosome localization

Paxillin localization at the MTOC has previously been reported in T lymphocyte cells (Herreros *et al.*, 2000). A detectable enrichment of endogenous paxillin at the centrosome was also observed in epithelial cells (MDA-MB-231 and U2OS) and of GFP-tagged paxillin expressed in paxillin–/– MEFs (Figure 5, A–C), where it showed a pattern similar to acetylated tubulin (Supplemental Figure S5A). To determine which domain of paxillin is responsible for its targeting to the centrosome, GFP-tagged wild-type and paxillin domain mutants were transfected into paxillin–/– MEFs. Interestingly, the GFP-paxillin ΔLD2 and ΔLD4 mutants and even the ΔPro mutant were each able to localize to the centrosome (Figure 5, B and C). However, we did not observe centrosome localization of the nonphosphorylatable paxillin (Y31/118F), suggesting that paxillin phosphorylation is required for its localization to this organelle (Figure 5, B and C). Interestingly and in support of these observations, the potential phospho-mimetic Y31/118E mutant of paxillin localized weakly to the centrosome (Supplemental Figure S5B).

Paxillin localizes primarily to FAs (Turner *et al.*, 1990; Zaidel-Bar *et al.*, 2007). To address the potential importance of FA signaling in paxillin localization to the centrosome, the GFP-paxillin–expressing paxillin–/– MEFs were plated on poly-L-lysine (PLL) to prevent the formation of FAs (Schottelndreier *et al.*, 1999). The absence of FAs was evident from the lack of GFP-paxillin localization at the cell periphery (Figure 5D) and also the absence of vinculin localization (Supplemental Figure S5H). Somewhat unexpectedly, in the paxillin–/– MEFs plated on PLL and transfected with wild-type GFP-paxillin, not only were FAs dispensable for centrosomal localization of paxillin (Figure 5D), but also centriole cohesion (Figure 5D and Supplemental Figure S5C), Golgi fragmentation (Supplemental Figure S5, D and E), and MT acetylation were rescued (Supplemental Figure S5, F and G).

Paxillin–/– MEFs were also transfected with GFP-paxillin mutated on both the LIM2 and LIM3 domains (C411/470A) to suppress its FA targeting when plated on fibronectin (Brown *et al.*, 1996). Expression of this mutant resulted in very limited FA localization as compared with vinculin (Supplemental Figure S5I). However, consistent with the results obtained by seeding the cells on PLL, this mutant targeted effectively to the centrosome (Figure 5E). Together, these data provide the first report of paxillin centrosomal localization in epithelial and fibroblast cells that is dependent on its phosphorylation at Y31/118 and independent of paxillin localization to FAs or FA signaling.

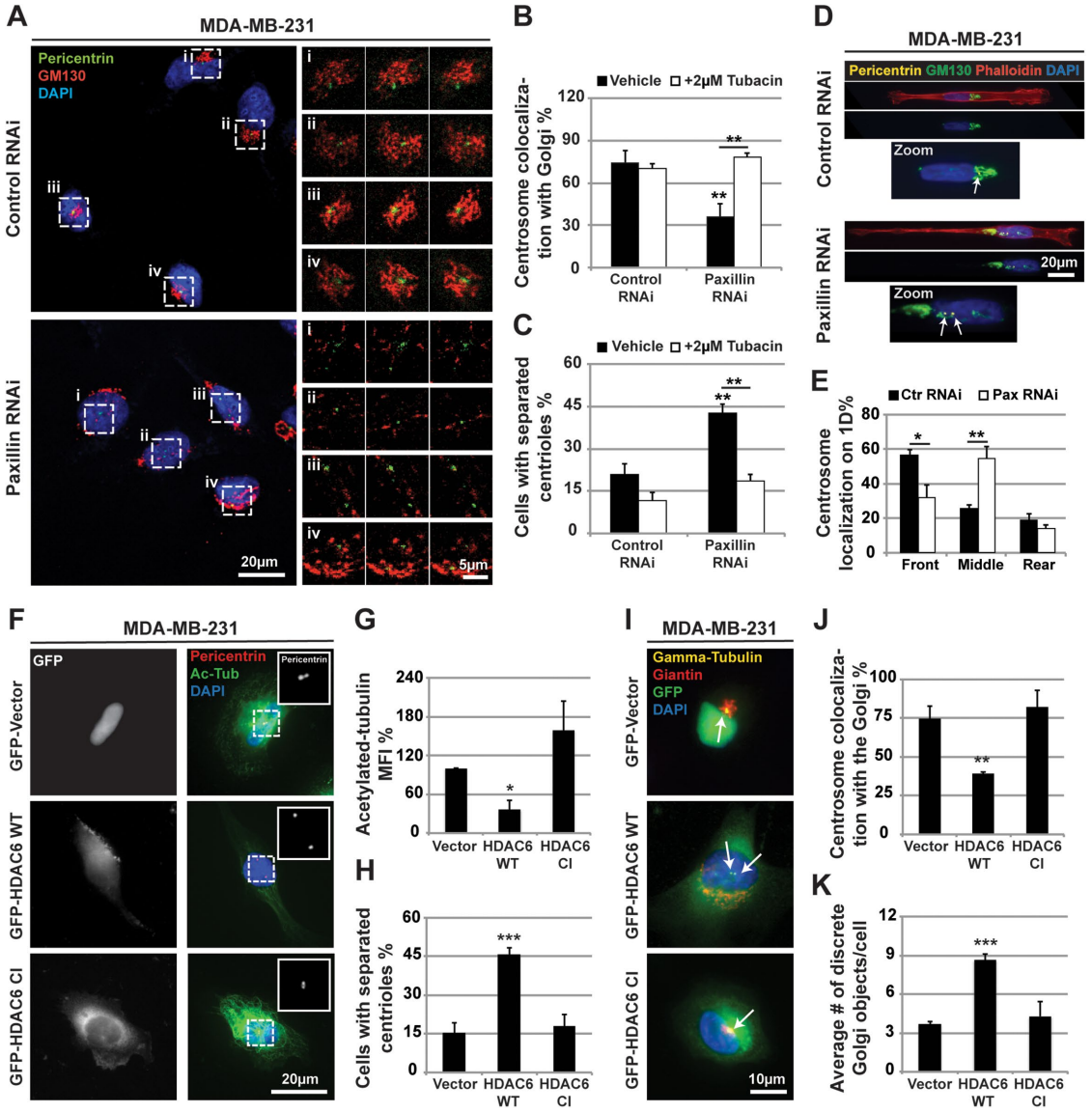

FIGURE 3: Paxillin is required for pericentrosomal Golgi localization and centrosome cohesion through HDAC6 inhibition. (A) Representative images of the Golgi (GM130) and centrosome (pericentrin) localization in MDA-MB-231 cells treated with control or paxillin RNAi and 2 μM tubacin for 4 h before fixation, as indicated. Boxed regions were used for the zoom of single slices of Z-stacks. (B) The percentage of cells with colocalized centrosome and Golgi and (C) the percentage of cells with separated centrioles (>1 μm between the centrioles). $n > 60$ cells. (D) Representative images and (E) quantification of the Golgi and centrosome localization (as indicated by the arrows) in cells plated on 1D fibronectin lines. $n > 50$ cells. (F) Representative images of parental MDA-MB-231 cells transfected with GFP-tagged wild-type (WT) or catalytically inactive mutants of HDAC6 and (G) quantification of acetylated tubulin mean fluorescence intensity (MFI) along with (H) quantification of cells with separated centrioles (>1 μm between the centrioles). $n > 30$ cells. (I) Representative images of the Golgi (Giantin) and centrosome (Gamma-tubulin) in MDA-MB-231 cells transfected with GFP-tagged constructs as indicated. Arrows indicate centrosome position. (J) Percentage of cells with colocalized centrosome and Golgi and (K) the average number of discrete Golgi objects per cell. $n > 30$ cells. Data are represented as the mean ± SEM from three individual experiments. Statistical significance was determined by Student's *t* test. *$p < 0.05$; **$p < 0.01$; ***$p < 0.001$.

FAK inhibition prevents paxillin localization to the centrosome and mimics the defects associated with paxillin depletion

FAK is one of the major mediators of cell–ECM signaling as well as paxillin phosphorylation at tyrosine 31/118 to create the binding sites for recruiting Src homology 2 domain–containing adapter and signaling proteins to FAs (Burridge *et al.*, 1992; Schaller, 2001; Brown and Turner, 2004; Supplemental Figure S2B). Moreover, paxillin depletion is known to cause a substantial reduction in FAK activity (Hagel *et al.*, 2002), which was confirmed in this study by blotting with the phospho-FAK antibody (pY397; Figure 6A). To assess the potential role of FAK in the accumulation of phospho-paxillin to the centrosome, the consequence of FAK inhibition was examined in the MDA-MB-231 cells using the FAK inhibitor (PF73228, 10 μM). In control cells, FAK inhibition (Figure 6A) caused a significant reduction in detectable levels of paxillin at the centrosome (Figure 6B).

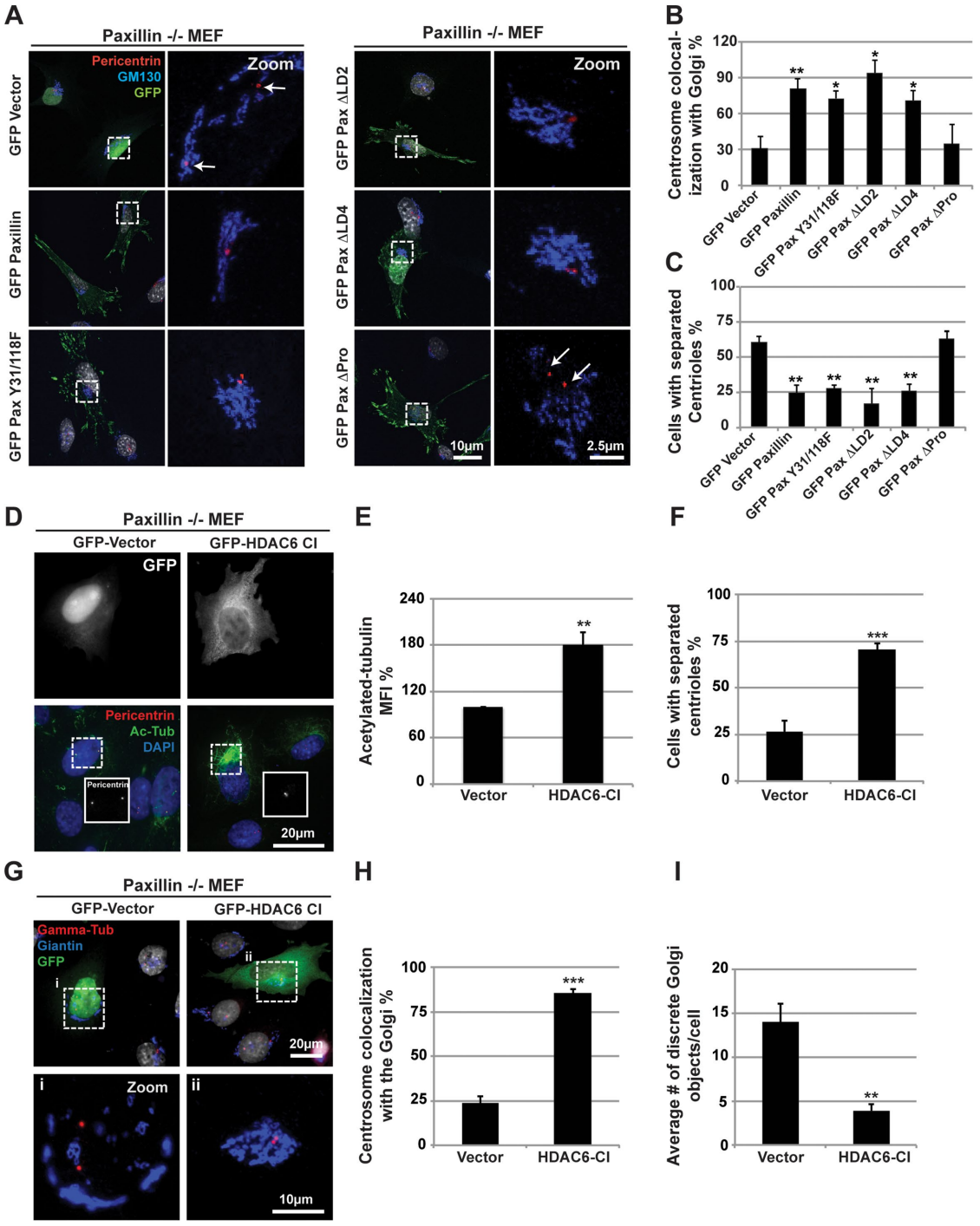

FIGURE 4: HDAC6 inhibition in the absence of paxillin is able to rescue Golgi and centrosome organization. (A) Representative images of Golgi and centrosome localization in paxillin–/– MEFs transfected with the GFP-paxillin constructs as indicated and plated on fibronectin-coated coverslips for 6 h before fixation and immunofluorescence staining. Arrows mark the positions of the two centrioles. (B) Quantification of cells with colocalized centrosome and Golgi and (C) cells with separated centrioles. $n > 50$ cells. (D) Representative images of paxillin–/– MEFs transfected with GFP-tagged vector or catalytically inactive mutant of HDAC6 and (E) quantification of acetylated tubulin MFI along with (F) quantification of cells with separated centrioles (>1 μm between the centrioles). $n > 30$ cells. (G) Representative images of the Golgi and centrosome in paxillin–/– MEFs transfected with GFP-tagged constructs as indicated. (H) The percentage of cells with colocalized centrosome and Golgi and (I) the average number of discrete Golgi objects per cell. $n > 30$ cells. Data are represented as the mean ± SEM from three individual experiments. Statistical significance was determined by Student's *t* test. *$p < 0.05$; **$p < 0.01$; ***$p < 0.001$.

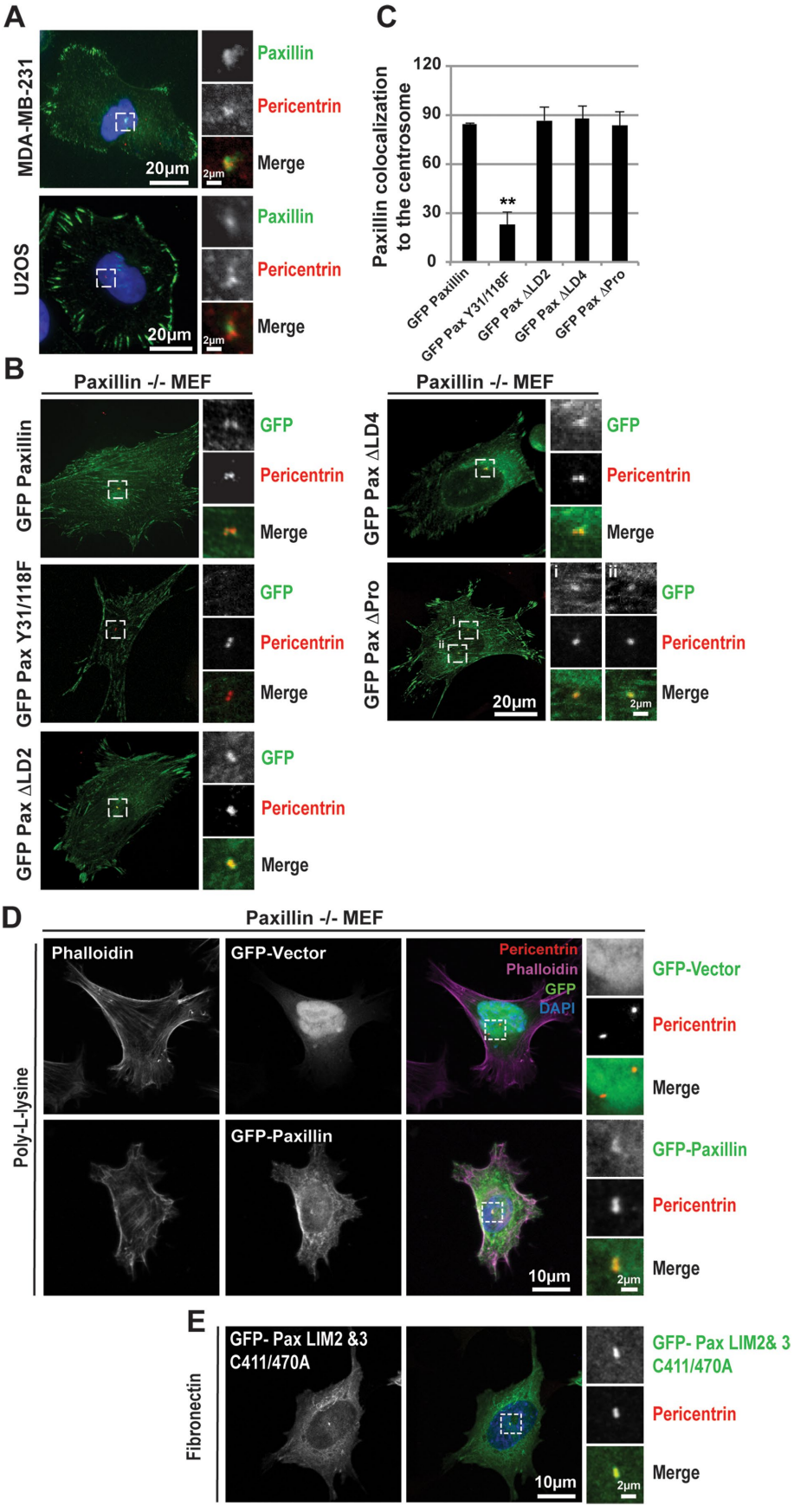

FIGURE 5: Phosphorylation of cytosolic paxillin is necessary for centrosome localization. (A) Representative images of centrosome (pericentrin) and endogenous paxillin colocalization in MDA-MB-231 and U2OS cells. (B) Representative images of GFP-paxillin wild-type and mutant localization to the centrosome in paxillin–/– MEFs as indicated. (C) Quantification of the percentage of cells with paxillin localization to the centrosome. $n > 30$ cells. (D) Representative images of centrosome cohesion and paxillin colocalization in the absence of FAs in paxillin–/– MEFs seeded on PLL transfected with GFP-vector or GFP-paxillin. (E) Representative image of centrosome and paxillin colocalization in paxillin–/– MEFs transfected with the GFP-paxillin LIM2/3 C411/470A mutant. Data are represented as the mean ± SEM from three individual experiments. Statistical significance was determined by Student's *t* test. $^{**}p < 0.01$.

Interestingly, FAK inhibition also resulted in centriole separation in ~40% of the cells (Figure 6C) as well as Golgi fragmentation and loss of Golgi pericentrosomal localization, comparable to paxillin RNAi treatment alone (Figures 6, D–F, and 3). These data suggest that FAK activity may coordinate with paxillin in the maintenance of both Golgi and centrosome structure.

It has been shown previously that FAK-mediated activation of RhoA can stimulate MT acetylation (Palazzo *et al.*, 2004). Therefore, activated FAK could regulate paxillin activity toward HDAC6 and thereby influence the level of acetylated tubulin. Consistent with a previous report (Palazzo *et al.*, 2004), FAK inhibition resulted in a substantial reduction of acetylated tubulin in MDA-MB-231 cells, as determined by both immunofluorescence imaging (Figure 6, G and H) and Western blot (Figure 6I), without affecting total MT distribution (unpublished data). Moreover, FAK inhibition reduced Golgi polarization in both the scratch wound assay and on 1D fibronectin lines (Figure 6, J–M), in agreement with previous studies (Tomar *et al.*, 2009; Serrels *et al.*, 2012). These data suggest an important role for FAK together with paxillin in the regulation of both MT acetylation and Golgi organization and positioning.

Paxillin and FAK collaboration is required for Golgi complex and centrosome organization

To further investigate the potential link between paxillin and FAK activity in the control of HDAC6 activity and MT acetylation, as well as centrosome and Golgi organization, paxillin–/– MEFs were transfected with either hemagglutinin (HA)-tagged wild-type FAK (WT FAK), or HA-tagged catalytically active FAK (SuperFAK), or HA-tagged

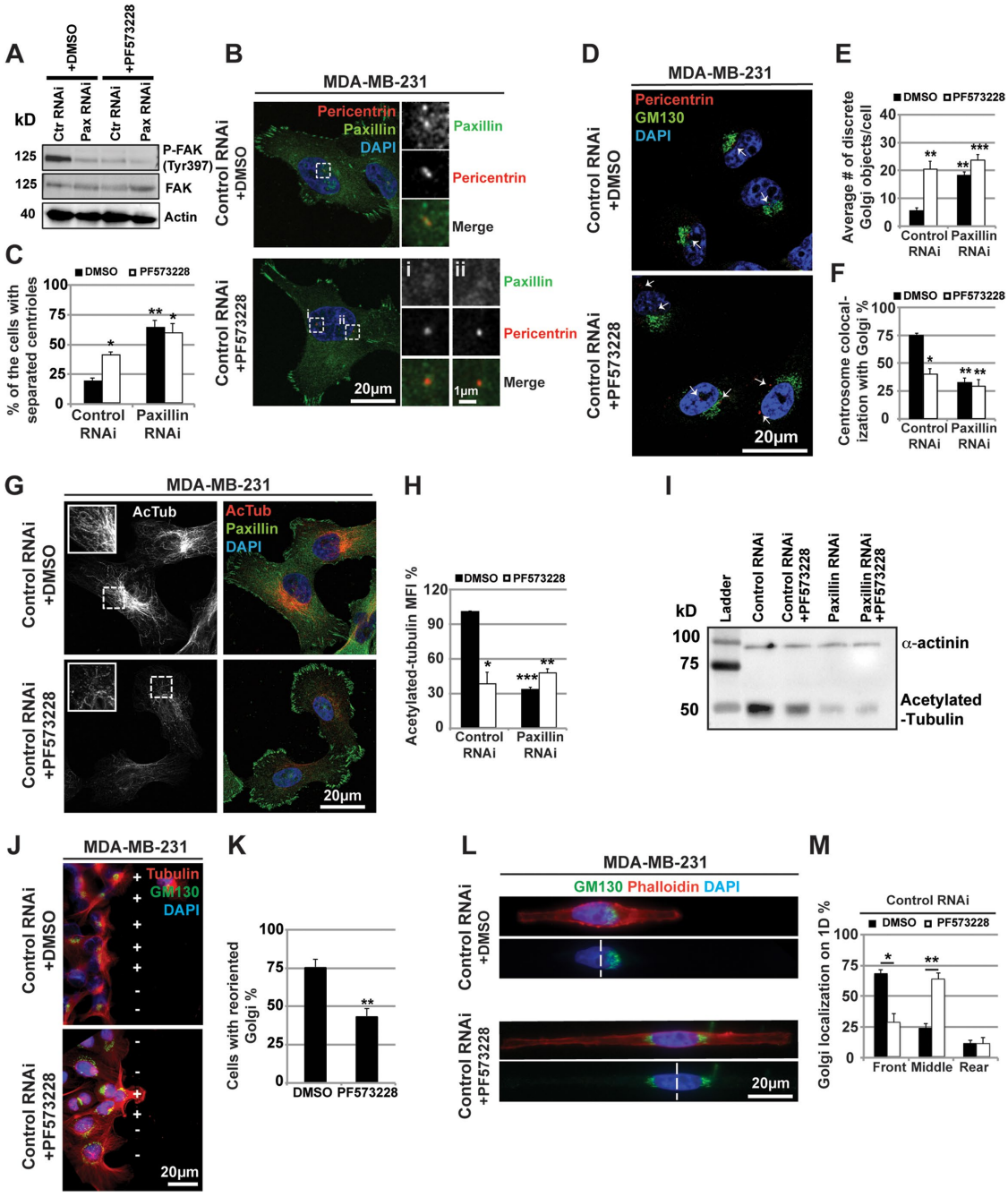

FIGURE 6: FAK inhibition prevents paxillin localization to the centrosome and mimics the defects associated with paxillin depletion. (A) Western blot indicating FAK activity (pY397) in MDA-MB-231 cells treated with control or paxillin RNAi, as indicated. FAK activity was inhibited using PF573228 (10 μM) for 1 h. DMSO, dimethyl sulfoxide. (B) Representative images of centrosome (pericentrin) and paxillin in MDA-MB-231 cells treated for 1 h with FAK inhibitor showing absence of paxillin localization to the centrosome after FAK inhibition along with (C) quantification of the percentage of the cells with separated centrioles (>1 μm between the centrioles). Centrosomes highlighted by white boxes are enlarged (right) with separated channels for better visualization. (D) Representative images of centrosome (pericentrin) and Golgi (GM130) localization in MDA-MB-231 cells treated for 1 h with FAK inhibitor and (E) quantification of discrete Golgi object number per cell and (F) quantification of percentage of cells with centrosome and Golgi colocalization. Arrows mark the positions of the two centrioles. (G) Representative images of acetylated tubulin in MDA-MB-231 cells treated for 1 h with FAK inhibitor along with (H) quantification of acetylated tubulin MFI per cell and (I) Western blot indicating a reduction in α-tubulin acetylation upon paxillin depletion and/or FAK inhibition. (J) Representative images and (K) analysis of Golgi reorientation 6 h after monolayer scrape wounding in MDA-MB-231 cells treated for 1 h before fixation with FAK inhibitor. The Golgi complex was scored as polarized (+) if it was positioned within a 90° sector facing the wound. (L) Representative images and (M) quantification of the Golgi localization on 1D fibronectin lines in MDA-MB-231 cells treated for 1 h with FAK inhibitor. See *Materials and Methods* for quantification detail. Data are represented as the mean ± SEM from three individual experiments. $n > 50$ cells. Statistical significance was determined by Student's t test. *$p < 0.05$; **$p < 0.01$; ***$p < 0.001$.

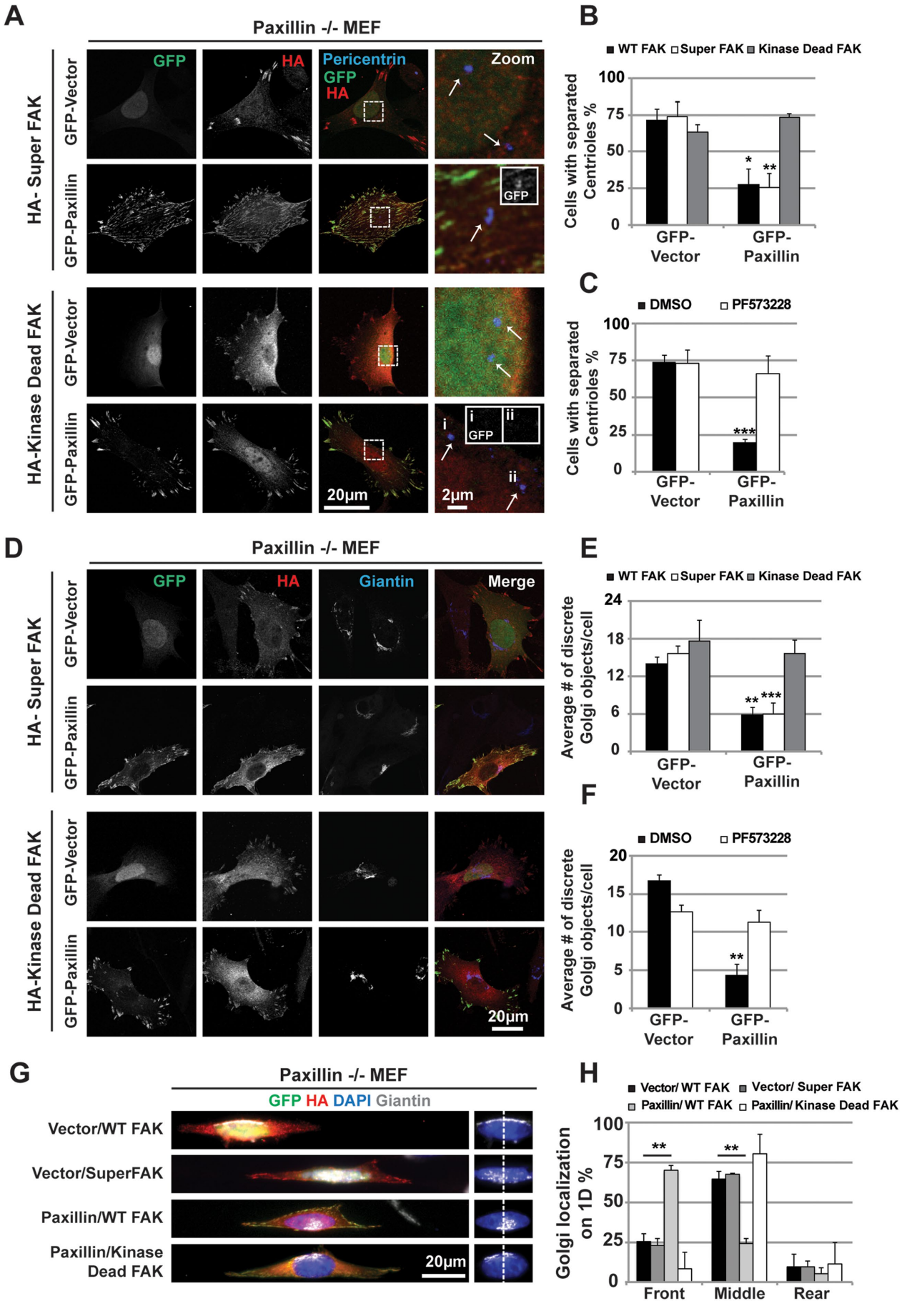
A
Paxillin -/- MEF
GFP
HA
Pericentrin
GFP
HA
Zoom
HA- Super FAK
GFP-Vector
GFP-Paxillin
HA-Kinase Dead FAK
GFP-Vector
GFP-Paxillin
GFP
i
ii
20µm
2µm
B
WT FAK Super FAK Kinase Dead FAK
Cells with separated Centrioles %
100
75
50
25
0
*
**
GFP-Vector
GFP-Paxillin
C
DMSO
PF573228
Cells with separated Centrioles %
100
75
50
25
0
***
GFP-Vector
GFP-Paxillin
D
Paxillin -/- MEF
GFP
HA
Giantin
Merge
HA- Super FAK
GFP-Vector
GFP-Paxillin
HA-Kinase Dead FAK
GFP-Vector
GFP-Paxillin
20µm
E
WT FAK Super FAK Kinase Dead FAK
Average # of discrete Golgi objects/cell
24
18
12
6
0
**
***
GFP-Vector
GFP-Paxillin
F
DMSO
PF573228
Average # of discrete Golgi objects/cell
20
15
10
5
0
**
GFP-Vector
GFP-Paxillin
G
Paxillin -/- MEF
GFP HA DAPI Giantin
Vector/WT FAK
Vector/SuperFAK
Paxillin/WT FAK
Paxillin/Kinase Dead FAK
20µm
H
Vector/ WT FAK
Vector/ Super FAK
Paxillin/ WT FAK
Paxillin/ Kinase Dead FAK
Golgi localization on 1D %
100
75
50
25
0
**
**
Front
Middle
Rear

catalytically inactive FAK (Kinase Dead FAK mutants) in combination with GFP-vector or GFP-paxillin. The expression of wild-type FAK or SuperFAK in paxillin–/– MEFs transfected with GFP-vector failed to rescue either centrosome separation (Figure 7, A and B) or Golgi fragmentation (Figure 7, D and E) and polarization (Figure 7, G and H). In contrast, when GFP-paxillin was cotransfected with wild-type or SuperFAK, results similar to those with GFP-paxillin alone were obtained (Figure 7, A–E), indicating that paxillin is required for FAK to control centrosome and Golgi organization. Furthermore, coexpression of GFP-paxillin with Kinase Dead FAK in paxillin–/– MEFs prevented the rescue of centriole separation, and the Golgi complex remained fragmented and unpolarized (Figure 7). Moreover, the GFP-paxillin failed to localize to the centrosome in Kinase Dead FAK–transfected cells (Figure 7A), demonstrating that paxillin function is also dependent on FAK kinase activity.

To further validate the functional relationship between paxillin and FAK, the paxillin–/– MEFs were also treated with FAK inhibitor (PF573228). In line with the results obtained using the Kinase Dead FAK mutant, FAK inhibition blocked the capacity of paxillin to rescue centrosome and Golgi organization and localization (Figure 7, C and F). Interestingly, and in agreement with the decrease of endogenous acetylated MTs after FAK inhibition in MDA-MB-231 cells (Figure 6, G–I), FAK inhibition with PF573228 also prevented the rescue of acetylated tubulin levels in paxillin–/– MEFs expressing either GFP-paxillin wild type or GFP-paxillin Y31/118F mutant (Supplemental Figure S6A). Similarly, Kinase Dead FAK cotransfection with GFP-paxillin resulted in suppressed levels of tubulin acetylation that were comparable to GFP-vector alone or GFP-vector cotransfected with SuperFAK (Supplemental Figure S6, B and C). These results indicate that paxillin cannot stimulate MT acetylation without FAK activity. Altogether, these results suggest new FA-independent roles for the paxillin-FAK cassette in coordinating various aspects of the cell polarization machinery.

Paxillin depletion causes a significant delay in anterograde vesicle trafficking

Polarization of the centrosome and Golgi complex and the subsequent asymmetric distribution of stable MT arrays promote effective protein trafficking to the leading edge of motile cells (Mellor, 2004). To investigate a potential role for paxillin in regulating protein trafficking, the temperature-sensitive mutant of GFP-labeled VSVG (vesicular stomatitis virus G; tsVSVG) was used to track anterograde transport from the endoplasmic reticulum (ER) to the plasma membrane (PM) in MDA-MB-231 cells transfected with either control or paxillin RNAi. At 40°C, the GFP-tsVSVG is misfolded and retained in the ER; however, upon shifting to 32°C, it becomes unfolded and traffics from the ER to the Golgi and then to the PM (Bergmann, 1989). In both control and paxillin-depleted MDA-MB-231 cells, immunofluorescence analysis of cells fixed at 40°C showed VSVG accumulation in the ER (Figure 8, A and B). However, upon transfer to 32°C, VSVG in control cells was colocalized with the Golgi complex after 10–15 min (Figure 8, A and C) and began to appear at the PM within 30 min (Figure 8, A and D). In contrast, in cells depleted of paxillin, VSVG trafficking from the ER to the Golgi and through the Golgi to the PM was significantly delayed, as compared with the control cells (Figure 8, A–D).

The analysis of VSVG trafficking was also performed in the paxillin–/– MEFs. Similar to observations in the MDA-MB-231 cells, RFP-vector– and RFP-paxillin–transfected cells accumulated and retained the GFP-tsVSVG cargo in the ER at 40°C (Supplemental Figure S7, A and B). However, after shifting the cells to the permissive temperature in the absence of paxillin, RFP-vector–transfected cells demonstrated an accumulation of large VSVG-containing vesicles around the Golgi at the various time points (Supplemental Figure S7, A and C), and in the majority of cells, VSVG arrived at the PM >1 h later (Supplemental Figure S7, A and D). In contrast, the expression of RFP-paxillin in the paxillin–/– MEFs restored normal trafficking. Within 15 min after the shift to 32°C, GFP-tsVSVG had left the ER and accumulated in the perinuclear Golgi (Supplemental Figure S7, B and C) and could also be detected at the PM within 30 min (Supplemental Figure S7, B and D). Taken together, these results demonstrate that paxillin is necessary for efficient anterograde cargo trafficking through the Golgi complex to the PM.

DISCUSSION

One of the major characteristics associated with directional cell migration is the establishment of front–rear polarization (Yadav *et al.*, 2009). Of importance, the FA adaptor protein paxillin contributes to persistent cell migration through maintaining the coordination of cell protrusion at the front and at the rear, in part by regulating FA dynamics (Webb *et al.*, 2004). Recently, a novel interaction between paxillin and HDAC6, an MT deacetylase, has also been reported to regulate cell migration by modulating MT acetylation and Golgi complex integrity (Deakin and Turner, 2014). Data presented herein reveal additional roles for paxillin as a key regulator of several key aspects of cell polarization through its ability to modulate HDAC6 activity and MT acetylation in both normal embryonic fibroblasts and transformed breast tumor cells.

In addition to Golgi complex fragmentation, paxillin depletion was also shown to disrupt the reorientation of the two principal MTOCs, the centrosome and Golgi complex, toward the leading edge in both polarized 2D and 1D ECM environments (Figures 1, 2, and 3D and Supplemental Figure S4). Although a crucial role for the MT network in organization and repositioning of the centrosome and Golgi complex has previously been reported (Thyberg and Moskalewski, 1999; Rivero *et al.*, 2009; Rios, 2014), the data herein reinforce the importance of MT acetylation as a specific

FIGURE 7: Paxillin and FAK collaboration is required for Golgi complex and centrosome organization. (A) Representative images of centrosome (pericentrin) in paxillin–/– MEFs transfected with GFP- and HA-tagged paxillin or FAK constructs, as indicated. Arrows mark the positions of the two centrioles in the zoomed images. Inset images of the GFP channel indicate paxillin localization to the centrosome. (B, C) The percentage of paxillin–/– MEFs with separated centrioles after (B) transfection with FAK constructs, as indicated, or (C) treatment with FAK inhibitor (10 μM PF573228) for 1 h before fixation. (D) Representative images of Golgi (Giantin) in paxillin–/– MEFs transfected with the GFP-paxillin and HA-tagged FAK constructs. (E, F) The average number of discrete Golgi objects/cell in paxillin–/– MEFs (E) transfected with FAK mutants or (F) treated with FAK inhibitor (10 μM PF573228) for 1 h before fixation. (G) Representative images and (H) quantification of the Golgi localization on 1D fibronectin lines (5 μm) in paxillin–/– MEFs transfected with GFP- and HA-tagged paxillin or FAK constructs, as indicated. See *Materials and Methods* for quantification detail. Data are presented as the mean ± SEM from three individual experiments. $n > 20$ cells. Statistical significance was determined by Student's *t* test. *$p < 0.05$; **$p < 0.01$; ***$p < 0.001$.

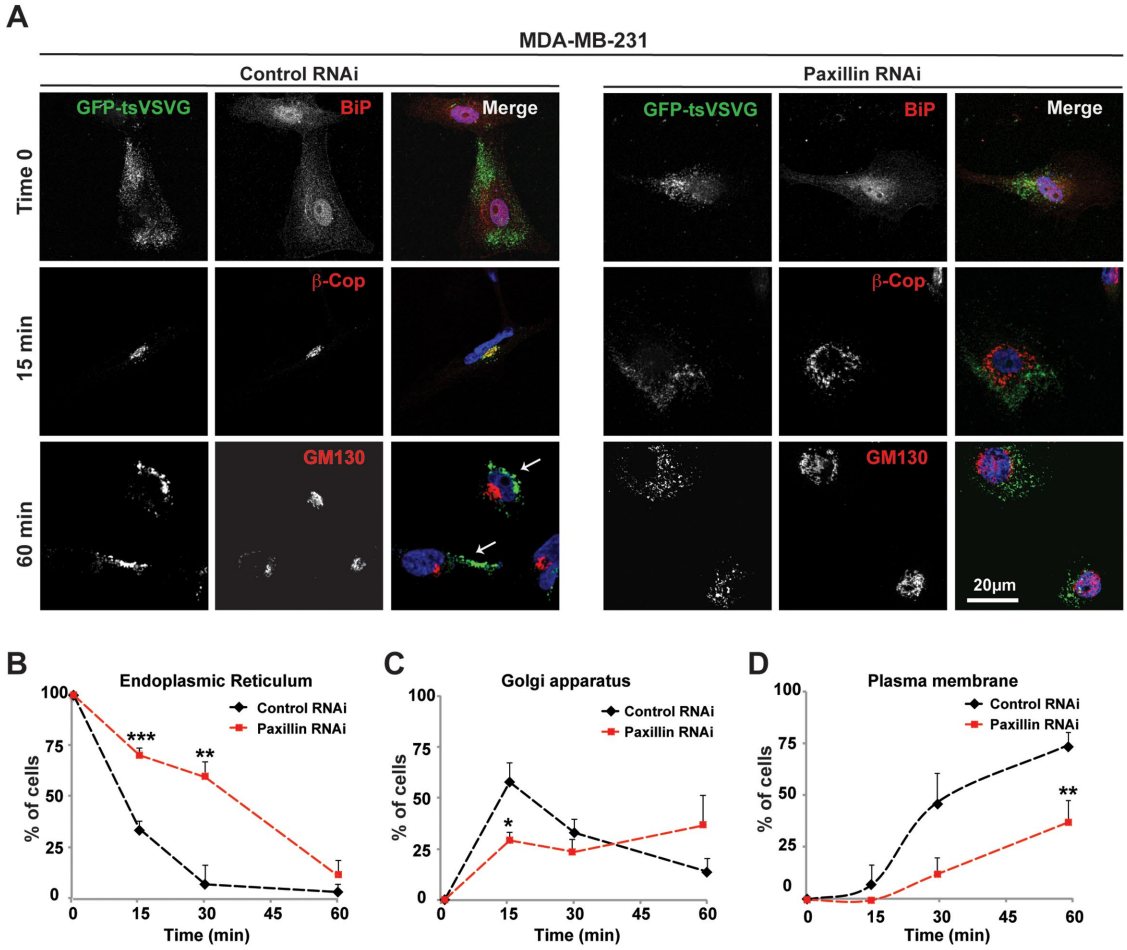

FIGURE 8: Paxillin depletion causes a significant delay in anterograde vesicle trafficking. (A) Time course of GFP-tsVSVG transport showing representative images of GFP-tsVSVG colocalization with BiP (ER marker), β-COP (ER to Golgi transport), and GM130 (*Cis*-Golgi marker) in fixed MDA-MB-231 cells treated with either control or paxillin RNAi. Images are from different time points after the switch from 40 to 32°C. Quantification of the percentage of cells in which GFP-tsVSVG was localized with (B) the ER, (C) the Golgi complex, and (D) the PM. Arrows mark the localization of GFP-tsVSVG at the PM. Data are represented as the mean ± SEM from three individual experiments. $n > 20$ cells. Statistical significance was determined by Student's *t* test. *$p < 0.05$; **$p < 0.01$; ***$p < 0.001$.

posttranslational modification in the regulation of these processes (Rios and Bornens, 2003; Miller *et al.*, 2009; Rivero *et al.*, 2009). These data further highlight the functional significance of paxillin as a modulator of MT acetylation via control of HDAC6 activity and introduce paxillin as a key regulator of both centrosome and Golgi polarization, further reinforcing the involvement of HDAC6 in the control of cell motility (Hubbert *et al.*, 2002; Haggarty *et al.*, 2003; Lafarga *et al.*, 2012; Deakin and Turner, 2014). Moreover, in the context of the loss of centrosome polarization after paxillin depletion (Figure 3D), it is of note that centrosome reorientation cannot be achieved without Golgi remodeling toward the leading edge (Bisel *et al.*, 2008), supporting a reciprocal relationship between the centrosome and Golgi apparatus.

Consistent with the shared role for the Golgi and centrosome in organizing a subset of stable MTs and the intimate structural and functional association between them and acetylated MTs (Chabin-Brion *et al.*, 2001; Keryer *et al.*, 2003; Hurtado *et al.*, 2011), two other major phenotypes were observed in paxillin-depleted cells, notably a loss of pericentrosomal Golgi organization and the loss of centriole cohesion (Figure 3, A–C). It is likely that these phenotypes also arise as a secondary effect of the reduction in MT acetylation after paxillin depletion, since the role of MTs in mediating a linkage between the Golgi stacks and the centrosome, as well as centriole cohesion, is well established (Sütterlin and Colanzi, 2010, Panic *et al.*, 2015). In agreement with this hypothesis, tubacin treatment or HDAC6 RNAi in paxillin knockdown MDA-MB-231 cells, as well as expression of all the paxillin mutants in paxillin–/– MEFs, except the mutant lacking the HDAC6-binding proline-rich domain, rescued both phenotypes to a similar extent as wild-type paxillin (Figures 3 and 4). Interestingly, centriole separation alone has also been shown to affect Golgi organization due to their reduced ability to nucleate MTs (Kushner *et al.*, 2014; Panic *et al.*, 2015), which leads to the hypothesis that paxillin-mediated loss of centriole cohesion could also be the reason for the Golgi fragmentation. Furthermore, it will be interesting to see whether paxillin depletion, by altering MT stability, impacts additional acetylated MT-related specific functions in the cells, for example, the enhanced binding and movement of MT motors, dynein and kinesin (Reed *et al.*, 2006; Theisen *et al.*, 2012).

We have also provided the first evidence of phospho-tyrosine (Y31/118)-dependent paxillin localization to the centrosome in both epithelial and fibroblast cells (Figure 5, A–C). Paxillin localization to the centrosome had previously only been observed in poorly adherent T lymphocyte cells (Herreros *et al.*, 2000) and in contributing to the reorientation and function of the MTOC at the immunological synapse (Robertson and Ostergaard, 2011). This localization was attributed to a direct interaction of the MTOC with the paxillin amino-terminus harboring paxillin Y31/118 and the LD motifs (Robertson and Ostergaard, 2011). In agreement with these findings, we have also shown that a paxillin LIM2/3 (C411/470A) mutant, which attenuates paxillin's interaction with both FAs and tubulin (Brown and Turner, 2002), still localizes to the centrosome in paxillin–/– MEFs (Figure 5E), thereby making the MTs themselves unlikely candidates for paxillin centrosomal recruitment. Although tyrosine phosphorylation of paxillin is critical for the localization and activities of paxillin at FAs (Brown and Turner, 2004; Zaidel-Bar *et al.*, 2007), a similar role for phospho-paxillin in regulation of centrosome functionality remains to be explored. Further studies will determine whether the scaffolding activity of paxillin is also necessary for the recruitment and anchoring of additional centrosomal molecules with specific functions, some of which, like paxillin, also have previously identified roles at FAs. For example, GIT1 and its associated p21-activated kinase, as well as FAK and Src kinases, are all FA proteins that accumulate at the centrosome at different times during the cell cycle to regulate the activity of various centrosomal proteins, such as Aurora A and PLK1 (Zhao *et al.*, 2005; Park *et al.*, 2009; Barretta *et al.*, 2016). Given the well-established physical and functional connection between paxillin and each of these proteins (Nayal *et al.*, 2006; Deakin and Turner, 2008) at FAs, it is tempting to speculate that paxillin may also act upstream to regulate their activity at the centrosome. It is of note that the accumulation of phospho-paxillin at the centrosome appears to be independent of its effects on MT stability and centrosome cohesion, as the GFP-paxillin ΔPro mutant can localize effectively to both separated centrioles (Figures 4A and 5B), highlighting the importance of stable MTs and the paxillin-HDAC6 axis in maintaining the centrioles in close proximity (Mimori-Kiyosue *et al.*, 2005; Wang *et al.*, 2008; Tang and Marshall, 2012).

Interestingly, by plating the cells on PLL to block FA formation (Schottelndreier *et al.*, 1999) or overexpression of the paxillin LIM2/3 domain mutant that cannot localize effectively to FAs (Brown *et al.*, 1996), we observed that paxillin centrosomal localization, as well as paxillin-dependent MT acetylation and the subsequent Golgi and centrosome organization, do not require FA signaling or paxillin targeting to the FAs (Figure 5, D and E, and Supplemental Figure S5, C–G). Although the paxillin LIM2 and LIM3 domains have been reported to bind tubulin and enhance MT targeting and stability at FAs (Brown and Turner, 2002; Efimov *et al.*, 2008), previous results obtained using a proximity ligation assay indicate a primarily cytoplasmic or peri-FA distribution of the paxillin-HDAC6 complex (Deakin and Turner, 2014), suggesting distinct roles for certain paxillin domains depending on the protein's cellular localization. These data together reinforce new roles for paxillin that are independent of its function at FAs.

Additionally, we have detailed a key interplay between paxillin and FAK in coordinating cell polarity (Figures 6 and 7). In this context, FAK was shown to function cooperatively with paxillin in the regulation of MT acetylation, which in turn is necessary for maintaining centrosome cohesion as well as Golgi pericentrosomal integrity and polarization. These data provide additional mechanistic context for previous reports describing a role for FAK in the control of Golgi reorientation and polarized cell motility (Mitra *et al.*, 2005; Tilghman *et al.*, 2005; Tomar *et al.*, 2009; Schaller, 2010). Interestingly, the activity of FAK was also found to be necessary for paxillin centrosomal localization, most likely via regulation of paxillin Y31/118 phosphorylation. However, whether direct interaction of FAK with paxillin is necessary for paxillin phosphorylation at the centrosome or whether paxillin localization occurs after FAK-dependent phosphorylation in the cytoplasm remains to be determined. Overall, these observations identify new roles for the paxillin-FAK signaling cassette and the concerted activity of both proteins in regulation of cell polarity. Moreover, in line with an emerging role of the actin cytoskeleton in influencing the position of the MTOC in polarized cells (Bornens, 2008; Hale *et al.*, 2011), it will be interesting to investigate whether paxillin and FAK signaling could act as a common pathway to regulate the interplay of the two cytoskeletal networks during cell polarization.

Finally, we have shown that an important functional consequence of paxillin depletion is that normal transport of tsGFP-VSVG from the ER to the Golgi and from the Golgi to the PM is significantly delayed (Figure 8). Indeed, it is well established that the polarized positioning of the centrosome and Golgi apparatus is a key prerequisite for the asymmetric distribution of stable MTs (Bisel *et al.*, 2008; Hurtado *et al.*, 2011) to increase the probability of directed delivery of vesicles and their cargo to the leading edge (Reed *et al.*, 2006; Bornens, 2012; Zhu and Kaverina, 2013). Furthermore, it has been shown that loss of polarized organization of the Golgi complex, as well as disconnection from the centrosome, impairs polarized trafficking in motile cells (Yadav *et al.*, 2009; Hurtado *et al.*, 2011; Millarte and Farhan, 2012). In addition, the absence of MTs has been shown to also deregulate the efficiency of vesicle trafficking and to cause the accumulation of Golgi proteins in the ER (Egea *et al.*, 2015). Because stable MT organization is implicated not only in vesicle trafficking toward the leading edge but also in internalization of cell-adhesion molecules such as integrins from the cell surface to promote FA turnover (Caswell and Norman, 2006; Fletcher and Rappoport, 2010; De Franceschi *et al.*, 2015), it will be important in future studies to evaluate whether paxillin activity is also required for receptor recycling.

In conclusion, our results define a new role for paxillin- and FAK-dependent MT acetylation in the control of pericentrosomal Golgi organization and reorientation, as well as in directed vesicular trafficking. In addition, these data show for the first time the FAK-dependent accumulation of phospho-paxillin at the centrosome, independent of integrin-mediated adhesions. Moreover, these data suggest the exciting potential for additional centrosome-specific functions of paxillin, such as in the control of spindle orientation in the stem cell niche (Yamashita, 2009), the control of centrosome duplication in normal cells, or the accumulation of supernumerary centrosomes in cancer cell populations (Pihan, 2013).

MATERIALS AND METHODS

Cell culture, RNAi, transfections, and inhibitors

The paxillin-null (paxillin–/–) MEFs were a gift from S. Thomas (Harvard Medical School, Cambridge, MA) and have been previously described (Hagel *et al.*, 2002). Human breast adenocarcinoma MDA-MB-231 and human bone osteosarcoma U2OS cell lines were purchased from the American Type Culture Collection. All cell lines were maintained at 37°C in a humidified incubator with 5% CO_2 and were grown in DMEM supplemented with 10% (vol/vol) heat-inactivated fetal bovine serum, 100 U/ml penicillin, 100 µg/ml streptomycin, and 2 mM L-glutamine. RNAi treatment was performed using Oligofectamine (Life Technologies, Grand Island, NY) according to

the manufacturer's instructions and analyzed 72 h after treatment. The following siRNA duplex oligonucleotides were used: paxillin, 5′-CCCUGACGAAAGAGAAGCCUA-3′ and 5′-UAGGCUUCUCUUUCGUCAGGG-3 from Thermo Fisher Scientific (Rockford, IL); HDAC6, 5′-CAUCCAAGUCCAUCGCAGAUU-3′ and 5′-UCUGCGAUGGACUUGGAUGUU-3′ (Kaluza *et al.*, 2011); and nontargeting control RNAi, 5′-ACUCUAUCUGCACGCUGACUU-3′ and 5′-GUCAGCGUGCAG AUAGAGUUU-3′ from Life Technologies (Grand Island, NY). Transient transfections with plasmids encoding wild-type and mutant paxillin, as well as FAK and HDAC6, were performed using Lipofectamine LTX (Invitrogen, Carlsbad, CA) following the manufacturer's instructions and as described in our previous studies (Brown *et al.*, 2005; Deakin and Turner, 2014). After transfection, cells were left for 24 h before fixation. To determine Golgi positioning relative to the nucleus, cells were infected with CFP-nucleus and RFP-Golgi (CellLight; Life Technologies, Grand Island, NY) containing baculovirus (2 µl per 10,000 cells) and incubated overnight at 37°C before live-cell imaging.

For HDAC6 inhibition, tubacin (Sigma Aldrich, St. Louis, MO) was used at a concentration of 2 µM for 4 h as described (Deakin and Turner, 2014). To inhibit FAK activity, PF573228 (Tocris Bioscience, Ellisville, MO) was added at a concentration of 10 µM as previously reported (Deakin and Turner, 2011). Synchronization of cells at the G1/S phase was accomplished by a double thymidine block. Cells were treated with 2 mM thymidine (Sigma Aldrich, St. Louis, MO) for 16 h, released into fresh media for 8 h, and again incubated with 2 mM thymidine for another 16 h before analysis.

Antibodies and immunofluorescence staining

The antibodies used in this study were as follows: mouse anti-paxillin (clones 165), mouse anti-acetylated tubulin (clone 6-11B-1), mouse anti–α-tubulin (clone DM1A), mouse anti–α-actinin (clone BM-75.2), mouse anti–γ-tubulin (clone GTU-88), mouse anti-vinculin (clone VIN-11-5), rabbit anti-fibronectin (F3648; Sigma Aldrich, St. Louis, MO), rabbit anti-paxillin (H-114), rabbit anti-GFP (Santa Cruz Biotechnology, Santa Cruz, CA), rabbit anti–p-FAK (Tyr397), rabbit anti–β-COP (Thermo Fisher, Rockford, IL), rabbit anti-pericentrin, mouse anti-HA.11 (clone 16B12; BioLegend, San Diego, CA), rabbit anti-BiP, mouse anti-actin (clone C4; EMD Millipore, Billerica, MA), rabbit anti-giantin (Covance, Princeton, NJ), mouse anti-GM130 (BD Biosciences, Franklin Lakes, NJ), rabbit anti-HDAC6 (Abcam), and rabbit anti–acetyl-α-tubulin (Cell Signaling Technology, Danvers, MA). Rhodamine- and Alexa Fluor 488–conjugated phalloidin (Life Technologies, Grand Island, NY) and 4′,6-diamidino-2-phenylindole (DAPI; Sigma Aldrich, St. Louis, MO) were used for visualization of F-actin and the cell nucleus, respectively.

Cells were cultured on fibronectin-coated coverslips (10 µg/ml) and were fixed with 4% paraformaldehyde for 20 min at room temperature or with ice-cold methanol for 10 min at –20°C to preserve actin filaments or MTs, respectively. Cells were fixed and permeabilized either simultaneously or sequentially with 0.1% Triton X-100 for 10 min. After extensive washes with phosphate-buffered saline (PBS), cells were blocked overnight with 3% bovine serum albumin and then stained with primary antibodies and counterstained with appropriate Alexa Fluor 488-, 550-, and 633-conjugated secondary antibodies (Thermo Fisher Scientific, Rockford, IL) and mounted in Gelvatol. For PLL coating, following manufacturer's instructions, the coverslips were soaked for 10 min in 0.01% (wt/vol) solution (70–150 kDa; Sigma Aldrich, St. Louis, MO) and then dried at room temperature for at least for 1 h before cell seeding.

Immunoblot analysis

For immunoblotting analyses, transfected cells were washed with PBS and then quickly lysed in sample buffer containing 20 mM Tris-HCl (pH 8), 10% glycerol, 2% SDS, and 0.1% bromophenol blue. Cell lysates were electrophoresed through SDS polyacrylamide gels and transferred to nitrocellulose (Life Science, St. Louis, MO). The membranes were blocked and probed with antibodies as described, and bound antibodies were visualized by chemiluminescence (SuperSignal West; Thermo Fisher Scientific, Rockford, IL) using a Chemidoc MP imaging system (Bio-Rad Laboratories).

Flow cytometry analysis

Trypsinized MDA-MB-231 cells were pelleted, washed in cold PBS, and fixed in 70% ice-cold ethanol overnight at 4°C. After fixation, cells were stained with 50 µg/ml propidium iodide in PBS containing 0.1% Triton X-100. Flow cytometry analysis was performed using a BD Fortessa flow cytometer. The data were plotted with Flowing software.

Wound-healing assay

Cells were seeded on fibronectin-coated coverslips, grown to confluence, and wounded by scratching with a P-200 pipette tip. The cells were then allowed to close the wound for ~6 h and were then processed for immunofluorescence staining with a Golgi marker (GM130 or giantin) and DAPI for nuclear visualization. The Golgi apparatus in the cells at the wound's edge were counted as polarized when the majority of the Golgi structure was located within a 90° angle toward the wound and nonpolarized if it was out of this sector.

Preparation of fibronectin-coated lines, micropatterns, and Golgi cohesion quantification

Fibronectin-coated lines and micropatterned substrates were prepared as previously described using deep-UV illumination (Tseng *et al.*, 2011). Briefly, a chrome-plated quartz photomask (Microtronics, Newtown, PA) was cleaned with water and wiped with Rain-X (ITW Global Brands, Houston, TX) before use in order to generate a hydrophobic surface. A polyacrylamide gel mixture (30% acrylamide and 2% bis-acrylamide) was polymerized for 1 h between the photomask and silanized coverslips at room temperature. Once the gel was polymerized, the photomask was placed in UVO-cleaner 342 (Jelight, Irvine, CA) and illuminated with UV light for 3 min. The coverslips were gently removed from the photomask and inverted over a drop of 5 mg/ml EDC (1-ethyl-3-(3-dimethylaminopropyl)carbodiimide hydrochloride; Thermo Fisher Scientific, Rockford, IL) and 10 mg/ml NHS (*N*-hydroxysuccinimide; Thermo Fisher Scientific, Rockford, IL) solution for 15 min, washed with HEPES (4-(2-hydroxyethyl)-1-piperazineethanesulfonic acid) buffer (pH 8.5), and incubated with buffer containing 10 µg/ml fibronectin for 1 h. The gels were then extensively washed in PBS before use.

For cells plated on either crossbows or lines, the position of the Golgi relative to the cell nucleus was classified into three groups. On crossbows, two intersecting perpendicular diagonal lines were drawn through the nucleus (Figure 1E). In the case of the lines, one vertical line was drawn dividing the nucleus into two equal parts (Figure 1G). We classified the Golgi on both crossbows and lines as "Front" and polarized when the Golgi structure was mostly localized in front of the nucleus toward the wider end, and a second group was referred to as "Rear" when the majority of Golgi fragments were positioned toward the narrower end, behind nucleus. The third group was classified as "Middle" when the Golgi fragments were mostly dispersed and could not be classified as having

either a front or rear position. For Golgi morphometric analyses, representative images were background subtracted, and the Golgi object number was quantified using the "analyze particles" plug-in in ImageJ.

tsVSVG trafficking assays

TsVSVG fused to GFP, pEGFPN1-VSVG, was purchased from Addgene (11912; Cambridge, MA) and has been described previously (Presley *et al.*, 1997). MDA-MB-231 or paxillin–/– MEFs plated on glass coverslips were infected with the adenovirus overnight in a 40°C incubator. Cells were subsequently transferred to 32°C to release VSVG from the ER for various time periods, as indicated, before fixation and immunofluorescence microscopy or were subjected to live-cell imaging.

Microscopy and live-cell imaging

Fluorescent images were recorded with either a Zeiss Axioskop2 Plus microscope fitted with a QImaging EXi Blue charge-coupled device camera using a Plan-Apochromat 20× or 40× numerical aperture (NA) objective or by using a Leica SP5 scanning confocal microscope with a high-contrast Plan-Apochromat 63×/1.40–0.60 oil-immersion objective and the associated software. Z-stacks were generated by taking optical sections at 0.2-µm intervals for centrosome analyses or at 0.5-µm intervals for the remaining analyses. The ImageJ software program (Image/Stacks/3D Project) was used for 3D reconstruction.

Glass-bottom 35-mm dishes (MatTek Corporation, Ashland, MA) were used for live-cell imaging. Seventy-two hours after RNAi knockdown or 24 h after transfection/infection, the cells were examined at 37°C, unless stated otherwise, in 5% CO_2 using a Nikon microscope (TE2000) equipped with an environmental chamber and automated stage. Images were collected every 10 min for 4 h using an HCX Plan Fluotar 20 × 0.70 NA objective using Elements software (Nikon).

Statistical analysis

Data are represented as the mean ± SEM of experiments performed independently at least three times. To determine statistical significance, a Student's unpaired *t* test was applied to all experiments. Statistical significance was set at $p < 0.05$.

ACKNOWLEDGMENTS

This study is supported by grants from the National Institutes of Health (GM-047607 and CA-163296). We thank Heidi Henley (State University of New York [SUNY] Upstate Medical University, Syracuse, NY) for helpful discussions regarding centrosome biology, Patrick Oakes (University of Rochester) for his assistance with developing the micropatterning protocols, and Lisa Phelps of the SUNY Upstate flow cytometry core facility for assistance with cell sorting. We are grateful to Ian Forsythe for additional technical assistance and members of the Turner lab for helpful suggestions and discussions.

REFERENCES

Aldana-Masangkay GI, Sakamoto KM (2011). The role of HDAC6 in cancer. J Biomed Biotechnol 2011, 875824.

Arnette C, Efimova N, Zhu X, Clark GJ, Kaverina I (2014). Microtubule segment stabilization by RASSF1A is required for proper microtubule dynamics and Golgi integrity. Mol Biol Cell 25, 800–810.

Barretta ML, Spano D, D'Ambrosio C, Cervigni RI, Scaloni A, Corda D, Colanzi A (2016). Aurora-A recruitment and centrosomal maturation are regulated by a Golgi-activated pool of Src during G2. Nat Commun 31, 117277.

Bergmann JE (1989). Using temperature-sensitive mutants of VSV to study membrane protein biogenesis. Methods Cell Biol 32, 85–110.

Bisel B, Wang Y, Wei JH, Xiang Y, Tang D, Miron-Mendoza M, Yoshimura S, Nakamura N, Seemann J (2008). ERK regulates Golgi and centrosome orientation toward the leading edge through GRASP65. J Cell Biol 182, 837–843.

Bornens M (2008). Organelle positioning and cell polarity. Nat Rev Mol Cell Biol 9, 874–886.

Bornens M (2012). The centrosome in cells and organisms. Science 335, 422–426.

Brown MC, Perrotta JA, Turner CE (1996). Identification of LIM3 as the principal determinant of paxillin focal adhesion localization and characterization of a novel motif on paxillin directing vinculin and focal adhesion kinase binding. J Cell Biol 135, 1109–1123.

Brown MC, Turner CE (2002). Roles for the tubulin- and PTP-PEST-binding paxillin LIM domains in cell adhesion and motility. Int J Biochem Cell Biol 34, 855–863.

Brown MC, Turner CE (2004). Paxillin: adapting to change. Physiol Rev 84, 1315–1339.

Brown MC, Cary LA, Jamieson JS, Cooper JA, Turner CE (2005). Src and FAK kinases cooperate to phosphorylate paxillin kinase linker, stimulate its focal adhesion localization, and regulate cell spreading and protrusiveness. Mol Biol Cell 16, 4316–4328.

Burakov A, Nadezhdina E, Slepchenko B, Rodionov V (2003). Centrosome positioning in interphase cells. J Cell Biol 162, 963–969.

Burridge K, Turner CE, Romer LH (1992). Tyrosine phosphorylation of paxillin and pp125FAK accompanies cell adhesion to extracellular matrix: a role in cytoskeletal assembly. J Cell Biol 119, 893–903.

Burute M, Prioux M, Blin G, Truchet S, Letort G, Tseng Q, Bessy T, Lowell S, Young J, Filhol O, Théry M (2016). Polarity reversal by centrosome repositioning primes cell scattering during epithelial-to-mesenchymal transition. Dev Cell 23, 168–184.

Caswell PT, Norman JC (2006). Integrin trafficking and the control of cell migration. Traffic 7, 4–21.

Chabin-Brion K, Marceiller J, Perez F, Settegrana C, Drechou A, Durand G, Pous C (2001). The Golgi complex is a microtubuleorganizing organelle. Mol Biol Cell 12, 2047–2060.

Conduit PT, Wainman A, Raff JW (2015). Centrosome function and assembly in animal cells. Nat Rev Mol Cell Biol 16, 611–624.

De Franceschi N, Hamidi H, Alanko J, Sahgal P, Ivaska J (2015). Integrin traffic—the update. J Cell Sci 128, 839–852.

Deakin NO, Turner CE (2008). Paxillin comes of age. J Cell Sci 121, 2435–2444.

Deakin NO, Turner CE (2011). Distinct roles for paxillin and Hic-5 in regulating breast cancer cell morphology, invasion, and metastasis. Mol Biol Cell 22, 327–341.

Deakin NO, Ballestrem C, Turner CE (2012). Paxillin and Hic-5 interaction with vinculin is differentially regulated by Rac1 and RhoA. PLoS One 7, e37990.

Deakin NO, Turner CE (2014). Paxillin inhibits HDAC6 to regulate microtubule acetylation, Golgi structure, and polarized migration. J Cell Biol 206, 395–413.

Doyle AD, Wang FW, Matsumoto K, Yamada KM (2009). One-dimensional topography underlies three-dimensional fibrillar cell migration. J Cell Biol 184, 481–490.

Efimov A, Schiefermeier N, Grigoriev I, Ohi R, Brown MC, Turner CE, Small JV, Kaverina I (2008). Paxillin-dependent stimulation of microtubule catastrophes at focal adhesion sites. J Cell Sci 15, 196–204.

Egea G, Serra-Peinado C, Gavilan MP, Rios RM (2015). Cytoskeleton and Golgi-apparatus interactions: a two-way road of function and structure. Cell Health Cytoskeleton 7, 37–54.

Etienne-Manneville S (2013). Microtubules in cell migration. Annu Rev Cell Dev Biol 29, 471–499.

Fletcher SJ, Rappoport JZ (2010). Moving forward: polarized trafficking in cell migration. Trends Cell Biol 20, 71–78.

Ganai SA (2017). Small-molecule modulation of HDAC6 activity: The propitious therapeutic strategy to vanquish neurodegenerative disorders. Curr Med Chem, doi: 10.2174/0929867324666170209104030.

Hagel M, George EL, Kim A, Tamimi R, Opitz SL, Turner CE, Imamoto A, Thomas SM (2002). The adaptor protein paxillin is essential for normal development in the mouse and is a critical transducer of fibronectin signaling. Mol Cell Biol 22, 901–915.

Haggarty SJ, Koeller KM, Wong JC, Grozinger CM, Schreiber SL (2003). Domain-selective small-molecule inhibitor of histone deacetylase 6 (HDAC6)-mediated tubulin deacetylation. Proc Natl Acad Sci USA 100, 4389–4394.

Hale CM, Chen WC, Khatau SB, Daniels BR, Lee JS, Wirtz D (2011). SMRT analysis of MTOC and nuclear positioning reveals the role of EB1 and LIC1 in single-cell polarization. J Cell Sci 124, 4267–4285.
Herreros L, Rodriguez-Fernandez JL, Brown MC, Alonso-Lebrero JL, Cabanas C, Sanchez-Madrid F, Longo N, Turner CE, Sánchez-Mateos P (2000). Paxillin localizes to the lymphocyte microtubule organizing center and associates with the microtubule cytoskeleton. J Biol Chem 275, 26436–26440.
Hoppeler-Lebel A, Celati C, Bellett G, Mogensen MM, Klein-Hitpass L, Bornens M, Tassin AM (2007). Centrosomal CAP350 protein stabilises microtubules associated with the Golgi complex. J Cell Sci 120, 3299–3308.
Hubbert C, Guardiola A, Shao R, Kawaguchi Y, Ito A, Nixon A, Yoshida M, Wang XF, Yao TP (2002). HDAC6 is a microtubule-associated deactylase. Nature 417, 455–458.
Hurtado L, Caballero C, Gavilan MP, Cardenas J, Bornens M, Rios RM (2011). Disconnecting the Golgi ribbon from the centrosome prevents directional cell migration and ciliogenesis. J Cell Biol 193, 917–933.
Jaffe AB, Hall A (2005). Rho GTPases: biochemistry and biology. Annu Rev Cell Dev Biol 21, 247–269.
Kaluza D, Kroll J, Gesierich S, Yao TP, Boon RA, Hergenreider E, Tjwa M, Rössig L, Seto E, Augustin HG, *et al.* (2011). Class IIb HDAC6 regulates endothelial cell migration and angiogenesis by deacetylation of cortactin. EMBO J 30, 4142–4156.
Kanno K, Kanno S, Nitta H, Uesugi N, Sugai T, Masuda T, Wakabayashi G, Maesawa C (2012). Overexpression of histone deacetylase 6 contributes to accelerated migration and invasion activity of hepatocellular carcinoma cells. Oncol Rep 28, 867–873.
Keryer G, Di Fiore B, Celati C, Lechtreck KF, Mogensen M, Delouvee A, Lavia P, Bornens M, Tassin AM (2003). Part of Ran is associated with AKAP450 at the centrosome: involvement in microtubule-organizing activity. Mol Biol Cell 14, 4260–4271.
Kushner EJ, Ferro LS, Liu JY, Durrant JR, Rogers SL, Dudley AC, Bautch VL (2014). Excess centrosomes disrupt endothelial cell migration via centrosome scattering. J Cell Biol 206, 257–272.
Lafarga V, Aymerich I, Tapia O, Mayor F, Penela P (2012). A novel GRK2/HDAC6 interaction modulates cell spreading and motility. EMBO J 31, 856–869.
Lee M, Vasioukhin V (2008). Cell polarity and cancer: cell and tissue polarity as a non-canonical tumor suppressor. J Cell Sci 121, 1141–1150.
Matov A, Applegate K, Kumar P, Thoma C, Krek W, Danuser G, Wittmann T (2010). Analysis of microtubule dynamic instability using a plus-end growth marker. Nat Methods 7, 761–768.
Matsuyama A, Shimazu T, Sumida Y, Saito A, Yoshimatsu Y, Seigneurin-Berny D, Osada H, Komatsu Y, Nishino N, Khochbin S, *et al.* (2002). In vivo destabilization of dynamic microtubules by HDAC6-mediated deacetylation. EMBO J 21, 6820–6831.
Mellor H (2004). Cell motility: Golgi signalling shapes up to ship out. Curr Biol 14, R434–R435.
Mellman I, Nelson WJ (2008). Coordinated protein sorting, targeting and distribution in polarized cells. Nat Rev Mol Cell Biol 9, 833–845.
Meraldi P, Nigg EA (2001). Centrosome cohesion is regulated by a balance of kinase and phosphatase activities. J Cell Sci 114, 3749–3757.
Millarte V, Farhan H (2012). The Golgi in cell migration: regulation by signal transduction and its implications for cancer cell metastasis. Sci World J 2102, 498278.
Miller PM, Folkmann AW, Maia AR, Efimova N, Efimov A, Kaverina I (2009). Golgi-derived CLASP-dependent microtubules control Golgi organization and polarized trafficking in motile cells. Nat Cell Biol 11, 1069–1080.
Mimori-Kiyosue Y, Grigoriev I, Lansbergen G, Sasaki H, Matsui C, Severin F, Galjart N, Grosveld F, Vorobjev I, Tsukita S, *et al.* (2005). CLASP1 and CLASP2 bind to EB1 and regulate microtubule plus-end dynamics at the cell cortex. J Cell Biol 168, 141–153.
Mitra SK, Hanson DA, Schlaepfer DD (2005). Focal adhesion kinase: in command and control of cell motility. Nat Rev Mol Cell Biol 6, 56–68.
Nayal A, Webb DJ, Brown CM, Schaefer EM, Vicente-Manzanares M, Horwitz AR (2006). Paxillin phosphorylation at Ser273 localizes a GIT1-PIX-PAK complex and regulates adhesion and protrusion dynamics. J Cell Biol 173, 587–589.
Palazzo AF, Eng CH, Schlaepfer DD, Marcantonio EE, Gundersen GG (2004). Localized stabilization of microtubules by integrin- and FAK-facilitated Rho signaling. Science 303, 836–839.
Panic M, Hata S, Neuner A, Schiebel E (2015). The centrosomal linker and microtubules provide dual levels of spatial coordination of centrosomes. PLoS Genet 11, e1005243.
Park AY, Shen TL, Chien S, Guan JL (2009). Role of focal adhesion kinase Ser-732 phosphorylation in centrosome function during mitosis. J Biol Chem 284, 9418–9425.
Petrie RJ, Doyle AD, Yamada KM (2009). Random versus directionally persistent cell migration. Nat Rev Mol Cell Biol 10, 538–549.
Pihan GA (2013). Centrosome dysfunction contributes to chromosome instability, chromoanagenesis, and genome reprograming in cancer. Front Oncol 3, 277.
Prager-Khoutorsky M, Lichtenstein A, Krishnan R, Rajendran K, Mayo A, Kam Z, Geiger B, Bershadsky AD (2011). Fibroblast polarization is a matrix-rigidity-dependent process controlled by focal adhesion mechanosensing. Nat Cell Biol 13, 1457–1465.
Presley JF, Cole NB, Schroer TA, Hirschberg K, Zaal KJ, Lippincott-Schwartz J (1997). ER-to-Golgi transport visualized in living cells. Nature 389, 81–85.
Raghavan S, Vaezi A, Fuchs E (2003). A role for αβ1 integrins in focal adhesion function and polarized cytoskeletal dynamics. Dev Cell 5, 415–427.
Reed NA, Cai D, Blasius TL, Jih GT, Meyhofer E, Gaertig J, Verhey KJ (2006). Microtubule acetylation promotes kinesin-1 binding and transport. Curr Biol 16, 2166–2172.
Rey M, Irondelle M, Waharte F, Lizarraga F, Chavrier P (2011). HDAC6 is required for invadopodia activity and invasion by breast tumor cells. Eur J Cell Biol 90, 128–135.
Ridley AJ, Schwartz MA, Burridge K, Firtel RA, Ginsberg MH, Borisy G, Parsons JT, Horwitz AR (2003). Cell migration: integrating signals from front to back. Science 302, 1704–1709.
Rieder CL, Faruki S, Khodjakov A (2001). The centrosome in vertebrates: more than a microtubule-organizing center. Trends Cell Biol 11, 413–419.
Rios RM, Bornens M (2003). The Golgi apparatus at the cell centre. Curr Opin Cell Biol 15, 60–66.
Rios RM (2014). The centrosome-Golgi apparatus nexus. Philos Trans R Soc Lond B Biol Sci 369, 20130462.
Rivero S, Cardenas J, Bornens M, Rios RM (2009). Microtubule nucleation at the cis-side of the Golgi apparatus requires AKAP450 and GM130. EMBO J 28, 1016–1028.
Robertson LK, Ostergaard HL (2011). Paxillin associates with the microtubule cytoskeleton and the immunological synapse of CTL through its leucine-aspartic acid domains and contributes to microtubule organizing center reorientation. J Immunol 187, 5824–5833.
Sanders AA, Kaverina I (2015). Nucleation and dynamics of golgiderived microtubules. Front Neurosci 9, 431.
Schaller MD (2001). Paxillin: a focal adhesion-associated adaptor protein. Oncogene 20, 6459–6472.
Schaller MD (2010). Cellular functions of FAK kinases: insight into molecular mechanisms and novel functions. J Cell Sci 123, 1007–1013.
Scheswohl DM, Harrell JR, Rajfur Z, Gao G, Campbell SL, Schaller MD (2008). Multiple paxillin binding sites regulate FAK function. J Mol Signal 3, 1.
Schottelndreier H, Mayr GW, Guse AH (1999). β1-integrins mediate Ca2+-signalling and T cell spreading via divergent pathways. Cell Signal 11, 611–619.
Schneider IC, Hays CK, Waterman CM (2009). Epidermal growth factor induced contraction regulates paxillin phosphorylation to temporally separate traction generation from de-adhesion. Mol Biol Cell 20, 3155–3167.
Serrels A, McLeod K, Canel M, Kinnaird A, Graham K, Frame MC, Brunton VG (2012). The role of focal adhesion kinase catalytic activity on the proliferation and migration of squamous cell carcinoma cells. Int J Cancer 15, 287–297131.
Sütterlin C, Colanzi A (2010). The Golgi and the centrosome: building a functional partnership. J Cell Biol 188, 621–628.
Tang N, Marshall WF (2012). Centrosome positioning in vertebrate development. J Cell Sci 125, 4951–4961.
Theisen U, Straube E, Straube A (2012). Directional persistence of migrating cells requires Kif1C-mediated stabilization of trailing adhesions. Dev Cell 23, 1153–1166.
Théry M (2010). Micropatterning as a tool to decipher cell morphogenesis and functions. J Cell Sci 123, 4201–4213.
Thyberg J, Moskalewski S (1999). Role of microtubules in the organization of the Golgi complex. Exp Cell Res 246, 263–279.

Tilghman RW, Slack-Davis JK, Sergina N, Martin KH, Iwanicki M, Hershey ED, Beggs HE, Reichardt LF, Parsons JT (2005). Focal adhesion kinase is required for the spatial organization of the leading edge in migrating cells. J Cell Sci 118, 2613–2623.
Tomar A, Lim ST, Lim Y, Schlaepfer DD (2009). A FAK–p120RasGAP–p190RhoGAP complex regulates polarity in migrating cells. J Cell Sci 122, 1852–1862.
Tseng Q, Wang I, Balland M (2011). A new micropatterning method of soft substrates reveals that different tumorigenic signals can promote or reduce cell contraction levels. Lab Chip 11, 2231–2240.
Turner CE, Glenney JR Jr, Burridge K (1990). Paxillin: a new vinculin-binding protein present in focal adhesions. J Cell Biol 111, 1059–1068.
Vinogradova T, Raia P, Grimaldi AD, Loncarek J, Miller PM, Yampolsky D, Magidson V, Khodjakov A, Mogliner A, Kaverina I (2012). Concerted effort of centrosomal and Golgi-derived microtubules is required for proper Golgi complex assembly but not for maintenance. Mol Biol Cell 23, 820–833.
Wang W, Chen L, Ding Y, Jin J, Liao K (2008). Centrosome separation driven by actin-microfilaments during mitosis is mediated by centrosome-associated tyrosine-phosphorylated cortactin. J Cell Sci 121, 1334–1343.
Webb DJ, Donais K, Whitmore LA, Thomas SM, Turner CE, Parsons JT, Horwitz AF (2004). FAK-Src signalling through paxillin, ERK and MLCK regulates adhesion disassembly. Nat Cell Biol 6, 154–161.
Yadav S, Puri S, Linstedt AD (2009). A primary role for Golgi positioning in directed secretion, cell polarity, and wound healing. Mol Biol Cell 20, 1728–1736.
Yamashita YM (2009). The centrosome and asymmetric cell division. Prion 3, 84–88.
Zaidel-Bar R, Itzkovitz S, Ma'ayan A, Iyengar R, Geiger B (2007). Functional atlas of the integrin adhesome. Nat Cell Biol 9, 858–867.
Zhao ZS, Lim JP, Ng YW, Lim L, Manser E (2005). The GIT-associated kinase PAK targets to the centrosome and regulates Aurora-A. Mol Cell 20, 237–249.
Zhang L, Sheng S, Qin C (2013). The role of HDAC6 in Alzheimer's disease. J Alzheimers Dis 33, 283–295.
Zhu X, Kaverina I (2013). Golgi as an MTOC: making microtubules for its own good. Histochem Cell Biol 140, 361–367.